



Optimization of tensile strength of PLA/clay/rice husk composites using Box-Behnken design

Vianney Andrew Yiga¹ · Michael Lubwama^{1,2} · Sinja Pagel³ · Peter Wilberforce Olupot¹ · Johannes Benz³ · Christian Bonten³

Received: 14 July 2021 / Revised: 15 September 2021 / Accepted: 16 September 2021
© The Author(s) 2021

Abstract

It is extremely important to save costs and time while enhancing accuracy in experimentation. However, no study has utilized response surface methodology (RSM) to obtain the effects of independent parameters on properties of PLA/clay/rice husk composites. This study focused on optimization of tensile strength of fiber-reinforced polylactic acid (PLA) composites. RSM using Box-Behnken design (BBD) was used to determine optimum blending parameters of the developed composites. Fiber-reinforced PLA composites were prepared using compression molding. Rice husk fiber and clay filler were used to enhance tensile properties of PLA. Five factors, namely, clay filler loading (1–5 wt.%), rice husk fiber loading (10–30 wt.%), alkali concentration (0–4 wt.%), rice husk variety (K85, K98), and alkali type (NaOH, Mg(OH)₂) were varied with 68 individual experiments. Tensile tests were carried out according to ASTM D638 standards. ANOVA results revealed that the quadratic models best fit the tensile strength response, with filler loading and fiber loading factors as the most significant model terms. Interaction effects were more predominant than linear and quadratic effects. The developed models used to determine maximum tensile strengths of PLA/clay/rice husk composites were in close agreement with experimental findings (R^2 values of 0.9635, 0.9624, 0.9789, and 0.9731 for NaOH-modified K85 rice husks, Mg(OH)₂-modified K85 rice husks, NaOH-modified K98 rice husks, and Mg(OH)₂-modified K98 rice husks respectively). Individual optimal conditions were used to predict maximum tensile strengths in each set of developed composites. The predicted tensile strengths were 32.09 MPa, 33.69 MPa, 32.47 MPa, and 32.75 MPa for PLA/clay composites loaded with NaOH-modified K85 rice husks, Mg(OH)₂-modified K85 rice husks, NaOH-modified K98 rice husks, and Mg(OH)₂-modified K98 rice husks, respectively, which were very close to the obtained experimental values of 31.73 MPa, 33.06 MPa, 32.02 MPa, and 31.86 MPa respectively.

Keywords Box-Behnken design · Clay · Fiber-reinforced PLA · Optimization · Response surface methodology · Rice husks · Tensile strength

1 Introduction

Engineering and science efforts towards sustainable reinforcement of polymer matrices with natural fibers are increasing fast in recent times [1]. Natural fibers are

advantageous over their synthetic counterparts as reinforcement because they are low-cost, tough, non-abrasive, flexible during processing, and eco-friendly [2–6]. They can be extracted from various plant parts and classified accordingly [7]. Rice husks are natural fibers obtained by milling processes, constituting approximately 20% of total paddy rice [8, 9]. They are characterized by low density, low calorific value, and high ash content and contain about 35%, 25%, and 20% cellulose, hemicellulose, and lignin respectively [9, 10]. Rice husks are underutilized in Uganda and many other developing nations, due to limitations in methods necessary to convert them into useful products [11]. As such, majority of the rice husks generated by agricultural processing are often burned in open fields, a practice which creates negative environmental impacts [12–14].

✉ Vianney Andrew Yiga
vianney.yiga@mak.ac.ug

¹ Department of Mechanical Engineering, Makerere University, Kampala, Uganda

² Africa Center of Excellence in Materials, Product Development and Nanotechnology, Makerere University, Kampala, Uganda

³ Institut Für Kunststofftechnik, University of Stuttgart, Stuttgart, Germany

There is therefore urgent need to find suitable uses of rice husks since they are abrasive, low cost, lightweight, renewable, biodegradable, and universally available [8]. For example, rice husks can be suitably used as reinforcement in composites with polylactic acid (PLA) matrix to enhance PLA's tensile properties. Hamdan et al. [15] utilized MAPE compatibilizer in enhancing the tensile strength of rice husk fiber-reinforced PLA composites. Another study reported tensile strength of 0.05–0.5 MPa in PLA composites and that addition of 4 wt.% and 6 wt.% raw rice husk fiber increased the tensile strength by 95% and 43% respectively [16]. As such, these composites can be used as to develop components in Uganda's automotive industry [17, 18]. Use of natural fibers for enhancing tensile properties of PLA however depends on fiber loading, fiber surface modification effect, and filler loadings (like clay). Kovacevic et al. [19] studied the effect of fiber loading on tensile properties of fiber-reinforced PLA composites and reported increasing tensile strength of neat PLA by 136.80% at 30 wt.% fiber loading. Similarly, Wang et al. [20] and Yu et al. [21] reported that increase in fiber contents increased neat PLA's tensile strength. Sajna et al. [22] developed fiber-reinforced PLA composites with fiber loadings of 10, 20, 30, and 40 wt.%. They reported that 10 wt.% fiber loading reduced tensile strength of neat PLA but with subsequent increase in fiber loading to a 30 wt.% optimum, a marginal improvement was noted.

Aside from fiber loading as reported from the above studies, another aspect that affects tensile properties of PLA composites is adhesion between fiber material and PLA matrix. Poor adhesion between fibers and the matrix can be a great problem of natural fiber-reinforced PLA composites. The presence of impurities on surfaces of untreated natural fibers can cause ineffective bonding [23]. As such, PLA composites developed with untreated fibers may obtain poor tensile properties. For example, Jandas et al. [24] reported decreasing tensile strength of PLA with increase in untreated fiber material. This can however be overcome by chemical treatments to modify fibers' surfaces. This is because chemical treatment of agricultural fibers effectively removes fiber surface and offers a better fiber-matrix adhesion as well as interfacial loading transfer between the fiber and the matrix [25]. Jandas et al. [24] reported increasing tensile strength with NaOH and silane treatment of banana fibers. Sajna et al. [22] reported a 1.60% increase in PLA's tensile strength when fibers were silane treated as compared to untreated fiber-reinforced PLA composites. Hu et al. [26] reported that alkali modification (4%w/v) of fibers enhanced interfacial adhesion with PLA, which and increased the composites' tensile strength to 71.70 MPa compared to 54.50 MPa for the untreated fiber-reinforced PLA composites.

Another factor that can enhance tensile properties of fiber-reinforced PLA composites is clay incorporation.

Ramesh et al. [27] investigated the influence of 1, 2, and 3 wt.% clay filler loading on tensile properties of aloevera fiber-reinforced PLA composites. They reported that 1 wt.% clay loading increased tensile strength by 5.72%. A similar increase was also reported by Eng et al. [28]. Jandas et al. [24] presented the effect of clay loading (1, 3, and 5 wt.%) on tensile properties of banana fiber-reinforced PLA composites. They found that tensile strengths increased with addition of clay until the optimum point (3 wt.%). Similarly, Kumar et al. [29] reported an increase in neat PLA's tensile strength with 2.5 wt.% clay loading in flax fiber-reinforced PLA composites.

Based on the above factors, it is clear that a lot of effort goes into development of plastic composites. A traditional approach to experimental work for developing plastic composites is to vary one factor at a time, holding all other factors fixed but this is time consuming and unable to produce satisfactory results in a wide range of experimental settings [30]. As such, the complexity of developing PLA composites with the required tensile properties can be solved by employing response surface methodology (RSM) [31]. RSM is defined as a set of mathematical and statistical tools or techniques used to build some empirical models and explain relationships between factors and responses [32]. RSM is an effective tool for optimizing the PLA composites' tensile strength. From the literature review, as much as extensive research has been conducted to design experiments fiber-reinforced PLA composites, no study involved PLA composites based on rice husk fiber and clay filler. As such, there is a need to fill the knowledge gap on the tensile behavior of PLA/clay/rice husk composites. Therefore, the aim of this work was the characterization of different factors on the tensile strength of PLA/clay/rice husk composites. These factors included filler loading, fiber loading, alkali concentration, rice husk variety, and alkali type. To reduce the experimental complexity, the method of a Box-Behnken design was applied. The developed PLA composites were tested according to ASTM D638 standards at 25 °C.

2 Materials and methods

2.1 Materials

In this work, polylactic acid (4032D) matrix in pellet form was purchased from Huaian Ruanke Trade Co. Ltd, Huaian, China. It has a specific gravity 1.24 g/cm³ and melt flow index (MFI) of 7 g/10 min (210 °C/2.16 kg). Rice husks (K98 and K85) were obtained from Tororo district in Eastern Uganda. The obtained rice husks contained 13% moisture content. Kaolin was collected from Buwambo clay deposits in Central Uganda. Magnesium hydroxide (Mg(OH)₂) (CAS number 2917-11-90) with a molecular weight of 58.53 g/

mol and sodium hydroxide (NaOH) (CAS number 1310–73–2) with a molecular weight of 40 g/mol were both supplied by Lab Access Uganda Ltd, Kampala, Uganda. The research was carried out at the Department of Mechanical Engineering, Makerere University Kampala in Uganda.

2.2 Methods

2.2.1 Surface modification

Part of the rice husks (50%) were used as received. This formed the unmodified rice husk samples. Alkaline surface modification was done for the other part of husks using Magnesium hydroxide (Mg(OH)₂) and sodium hydroxide (NaOH) to form modified rice husk samples. This was done to enhance adhesion between fiber and matrix materials [12, 33]. Alkali modification involved soaking 1000 g of rice husks in 2 wt.% and 4 wt.% concentrated solutions for 3.5 h at ambient temperature. A liquor ratio of 20:1 was used. Alkali modified rice husk samples were then washed in reverse osmosis water until a neutral pH was obtained. The samples were dried for 48 h at room temperature and then at oven-dried at 60 °C overnight to reduce their moisture contents to <5% before storage, in order to improve their adhesion with PLA during composite processing [12, 34]. Kaolin was used as received.

2.2.2 Design of experiments

Tensile strength was optimized using a standard response surface methodology design in design of experiments called Box-Behnken design (BBD). BBD is a spherical and revolving design that consists of a central point and middle points of the edges [35]. BBD is more efficient than central composite design, Doehlert design, and 3-level factorial design because Box-Behnken designs are rotatable and do not contain combinations for which all factors are simultaneously at their highest or lowest levels [36]. Clay filler loading, rice husk fiber loading, alkali concentration, rice husk variety, and alkali type were employed as the five input factors in this study. The numeric factors—filler loading, fiber loading, and alkali concentration—were elucidated in ranges of

1–5 wt.% [24], 10–30 wt.% [35, 37], and 0–4 wt.% [26], respectively, as shown in Table 1.

Using the Design-Expert software (version 13, Stat-Ease Inc., MN, USA), runs were planned in a randomized order so as to minimize the effects of the uncontrolled factors. The runs were obtained with three numeric factors (*k*₁) and five replicated central points (*c*_p). This produced 17 experimental trials, five of which were replicated at the central points (0,0,0) as shown in Table 2. Additionally, two categorical factors (*k*₂) including rice husk variety and alkali type having two levels each were added to the design. The experimental design therefore produced 68 total required experiments based on Eq. (1). A key assumption made is that all numeric factors are continuous, measurable and controllable by experiments.

$$N = (2k_1(k_1 - 1) + c_p) \times (k_2)^2 = ((2 \times 3)(3 - 1) + 5) \times (2)^2 = 68 \tag{1}$$

The influence of the three numeric factors on the tensile strength of PLA/clay composites loaded with NaOH-modified K85 rice husks, Mg(OH)₂-modified K85 rice husks, NaOH-modified K98 rice husks, and Mg(OH)₂-modified K98 rice husks can be modeled using a second-order polynomial shown in Eq. (2).

$$Y = \beta_0 + \sum_{j=1}^k \beta_j x_j + \sum_{i < j} \sum \beta_{ij} x_i x_j + \sum_{i=0}^k \beta_{jj} x_j^2 + e \tag{2}$$

where *Y* is the predicted response value (tensile strength), β_0 is the model constant, β_j is the linear coefficient, β_{ij} is the interaction coefficient, β_{jj} is the quadratic coefficients, *x* is the independent factors in coded values, *k* is the number of factors studied and optimized in the experiment, and *e* is the experimental error.

2.2.3 Preparation of fiber-reinforced PLA composites

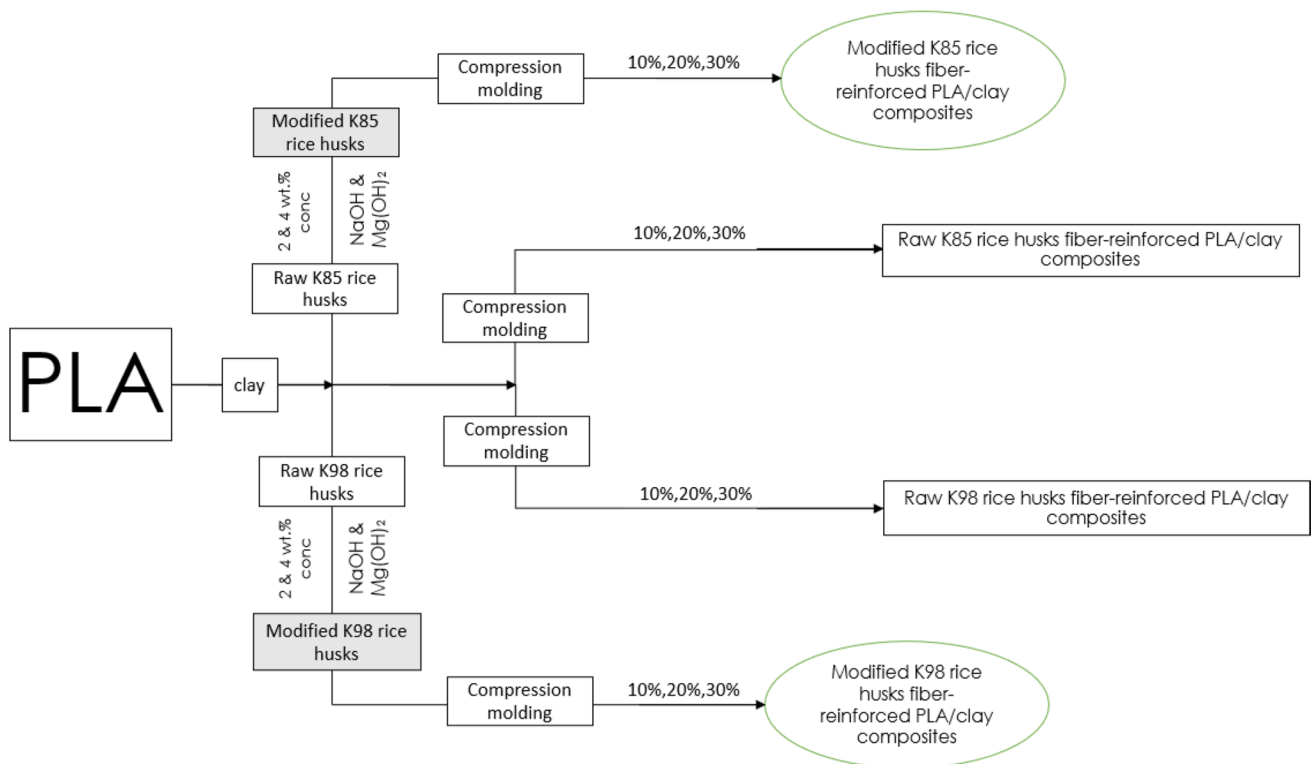
Fiber-reinforced PLA samples were produced as shown in Fig. 1. Prior to sample fabrication, PLA pellets, rice husks, and clay were held in an oven at 100 °C for 1 h. Rice husks and clay were then ground to ≤ 100 μm using a Retsch Planetary Ball mill PM 100 machine, Hann, Germany. The size reduction was done to ensure homogeneous

Table 1 Actual and coded factors for the Box-Behnken design

Factor	Type of factor	Code	Experimental value		
			Lower (−1)	Center (0)	Higher (+1)
Filler loading (wt.%)	Numeric	A	1	3	5
Fiber loading (wt.%)	Numeric	B	10	20	30
Alkali concentration (wt.%)	Numeric	C	0	2	4
Rice husk variety	Categoric	D	K85	-	K98
Alkali type	Categoric	E	NaOH	-	Mg(OH) ₂

Table 2 BBD and the experimental results

Run	Factors			NaOH-modified K85	Mg(OH) ₂ -modified K85	NaOH-modified K98	Mg(OH) ₂ -modified K98
	A (filler loading, wt.%)	B (fiber loading, wt.%)	C (alkali concentration, wt.%)	Response-tensile strength (MPa)			
1	1	10	2	22.64 ± 0.11	20.05 ± 1.09	21.15 ± 1.00	20.66 ± 1.86
2	5	20	4	32.08 ± 0.24	33.63 ± 0.09	32.44 ± 1.11	32.44 ± 0.32
3	3	20	2	24.81 ± 1.00	24.42 ± 0.00	24.61 ± 1.01	25.29 ± 0.00
4	1	30	2	25.58 ± 0.01	25.82 ± 0.28	26.51 ± 0.00	25.43 ± 0.12
5	3	20	2	24.67 ± 0.07	24.50 ± 1.01	25.72 ± 0.45	25.65 ± 0.22
6	5	10	2	25.51 ± 0.22	25.85 ± 0.00	25.79 ± 0.11	26.41 ± 0.11
7	5	20	0	22.91 ± 0.00	22.91 ± 0.41	22.37 ± 1.09	21.23 ± 0.71
8	1	20	0	30.22 ± 0.28	30.22 ± 0.52	29.19 ± 0.04	29.52 ± 0.11
9	3	20	2	24.23 ± 0.38	24.05 ± 0.12	25.35 ± 0.01	26.35 ± 0.42
10	3	10	4	25.59 ± 0.51	25.29 ± 0.00	25.09 ± 0.00	25.10 ± 0.14
11	3	20	2	25.53 ± 0.14	25.75 ± 0.01	25.87 ± 0.73	24.44 ± 0.05
12	5	30	2	26.43 ± 0.00	25.82 ± 0.00	27.61 ± 0.05	25.94 ± 0.11
13	3	20	2	24.31 ± 0.47	25.04 ± 0.83	25.52 ± 0.21	25.55 ± 0.02
14	1	20	4	19.54 ± 0.12	19.64 ± 0.87	21.15 ± 0.46	20.25 ± 0.22
15	3	30	4	22.80 ± 0.34	23.23 ± 0.31	23.56 ± 0.04	23.30 ± 0.17
16	3	30	0	29.29 ± 0.04	28.32 ± 0.00	27.38 ± 0.12	27.09 ± 0.00
17	3	10	0	23.27 ± 1.01	23.33 ± 1.19	21.17 ± 1.00	21.35 ± 0.81

**Fig. 1** Schematic diagram for fiber-reinforced PLA composite preparation

mixing of fiber, filler, and the PLA matrix materials. PLA was melted and mixed with ratios shown in Table 1 in a compression molding machine to obtain tensile strips. Uniform mixing between the filler, fiber, and matrix materials was achieved by a motor attached to the compression rig. The residence time for composite preparation at 195 °C during compression molding was 10 min. Compression was effected by use of a hand-screw jerk for 10 min under about 7 MPa loading. The developed tensile strips were then air-cooled for 10 min and stored before tensile testing.

$$Y_1 = 24.86 + 1.12A + 0.8862B - 0.710C + 4.96AC - 2.20BC + 0.8558C^2 \quad (3)$$

$$Y_2 = 25.00 + 1.56A + 1.08B - 1.45AB + 5.33AC - 1.76BC - 0.9309B^2 + 1.28C^2 \quad (4)$$

2.2.4 Tensile testing

Tensile tests for the developed PLA/clay/rice husk composite samples were performed according to ASTM D638 at room temperature (25 °C) using a Universal Testing Machine (Testometric FS300CT-2032, England, UK) with a 0–300 kN load cell range at a constant crosshead speed of 10 mm/min. Tests were conducted for three samples in each run and their average was used as the final result.

$$Y_3 = 25.39 + 1.28A + 1.48B - 0.8850AB + 4.53AC - 1.93BC + 0.9168A^2 - 1.07B^2 \quad (5)$$

3 Results and discussions

3.1 Model fitting for tensile strength

Box-Behnken design (BBD) was employed to create models between the numerical factors and the tensile strengths of the developed PLA/clay/rice husk composites based on their categorical factors. Table 2 shows the experimental design, together with corresponding experimental values for the response (tensile strength) for PLA/clay composites loaded with (i) NaOH-modified K85 rice husks, (ii) Mg(OH)₂-modified K85 rice husks, (iii) NaOH-modified K98 rice husks, and (iv) Mg(OH)₂-modified K98 rice husks.

Runs 3, 5, 9, 11, and 13 at the center point were employed to determine the experimental error and the reproducibility of the data. In order to obtain the best fit for each response set, the respective sequential model sum of squares values were considered. From each of these, the highest order polynomial, where the additional terms are significant, and the model is not aliased, was chosen. By applying multiple regression analysis to the response, four quadratic models were found to be the best fit of the response in each set. Analysis of variance (ANOVA) was used to ascertain significant interaction between factors and

tensile strengths based on their *p* values. *p* values less than 0.05 were considered significant while *p* values greater than 0.10 were non-significant and therefore removed and the final expressions of the best fitting models were deduced. For statistical significance of a model at a 95% confidence interval, the alpha value is 0.05 (5%). As such, for a given model to be satisfactory for use in estimating relationships between inputs and outputs, the probability value for a given factor must be very minimal (<0.05) [38, 39]. Additionally, factors' probability values greater than 0.1

(10%) are considered to be insignificant because above 0.1, the confidence interval is 90%, which cannot effectively justify model relationships [25, 40]. Therefore, the tensile strength response surface-reduced quadratic models corresponding to PLA/clay composites loaded with (i) NaOH-modified K85 rice husks (*Y*₁), (ii) Mg(OH)₂-modified K85 rice husks (*Y*₂), (iii) NaOH-modified K98 rice husks (*Y*₃), and (iv) Mg(OH)₂-modified K98 rice husks (*Y*₄) are given in Eqs. (3)–(6), respectively.

$$Y_4 = 25.64 + 1.27A + 1.03B - 1.31AB + 5.12AC - 1.88BC - 1.23B^2 \quad (6)$$

where *A* is filler loading (wt.%), *B* is fiber loading (wt.%), and *C* is alkali concentration (wt.%).

For these Equations, it is worth recalling that a positive sign in the regression equation represents the synergistic effect between parameters, whereas a negative sign indicates an antagonistic effect [41].

3.2 Analysis of variance for model statistical significance

The tensile strength results for the developed PLA/clay/rice husk composites were investigated using analysis of variance (ANOVA) in order to determine statistically significant factors in the fitted models for each set of PLA/clay composites (see Tables 3–6). Additionally, the models' lack-of-fits and the statistical significance of respective model coefficients were obtained.

The models' *F* values of 43.94, 32.87, 59.67, and 60.38 corresponding to the reduced quadratic models for tensile strength of PLA/clay composites loaded with

Table 3 ANOVA results for response surface-reduced quadratic model of tensile strength of PLA/clay composites loaded with NaOH-modified K85 rice husks

Source	Sum of squares	df	Mean square	F value	p value	
Model	141.34	6	23.5568	43.94	1.29E-06	Significant
A-filler loading	10.01	1	10.0128	18.68	0.001509	
B-fiber loading	6.28	1	6.2835	11.72	0.006507	
C-alkali concentration	4.03	1	4.0328	7.52	0.020732	
AC	98.51	1	98.5056	183.76	9.21E-08	
BC	19.40	1	19.4040	36.20	0.000129	
C ²	3.10	1	3.1021	5.79	0.03696	
Residual	5.36	10	0.5361			
Lack-of-fit	4.29	6	0.7144	2.66	0.181455	Not significant
Pure error	1.07	4	0.2686			
Cor total	146.70	16				
Mean	25.26 ± 0.73			R ²		0.9635
C.V.%	2.90			Adjusted R ²		0.9415
Adequate precision	25.888			Predicted R ²		0.8293

NaOH-modified K85 rice husks, Mg(OH)₂-modified K85 rice husks, NaOH-modified K98 rice husks, and Mg(OH)₂-modified K98 rice husks, respectively, imply that the developed models are significant (p values < 0.05). For each of the models, there is only a 0.01% chance that model F values this large could occur due to noise [42]. Moreover, lack-of-fits for the developed models were not significant relative to the pure error, further suggesting that the quadratic models adequately describe the functional relationships between experimental factors and respective tensile strengths [43]. Models' lack-of-fit F values of 2.66, 2.31, 1.68, and 0.82 corresponding to the reduced quadratic models for tensile strength of PLA/clay composites loaded with NaOH-modified K85 rice husks, Mg(OH)₂-modified K85 rice husks, NaOH-modified K98 rice husks, and Mg(OH)₂-modified K98 rice husks respectively show that there are 18.15%, 21.93%, 31.75%, and 60.77% chances, respectively, that lack-of-fit values occurred due to noise. Therefore, a non-significant lack-of-fit is good as the intention is for the model to fit so that it can adequately predict the response (tensile strength) [44, 45].

The tensile strength models were statistically inspected using lack-of-fit values. Lack-of-fits of the models' p values were 0.18, 0.22, 0.32, and 0.61 corresponding to the reduced quadratic models for tensile strength of PLA/clay composites loaded with NaOH-modified K85 rice husks, Mg(OH)₂-modified K85 rice husks, NaOH-modified K98 rice husks, and Mg(OH)₂-modified K98 rice husks respectively. It should be noted that the significant interaction between factors and tensile strength was evaluated based on the p values of the factors, and values greater than 0.10 were removed to improve the models. As shown in Table 3, A, B, C, AC, BC, and C² are significant terms for the tensile strength surface-reduced quadratic model for PLA/clay composites loaded with NaOH-modified K85 rice husks. Among these, the

interactive effect between filler loading and alkali concentration (F value 183.76) was found to be the most significant influencing factor. This is possibly due to the fact that alkali modification leads to better interaction, compatibility, and adhesion between both clay filler and NaOH-modified K85 rice husks to the PLA matrix, thereby increasing composites' tensile strength [27]. This was followed by the interactive effect between fiber loading and alkali concentration (F value 36.20). The least significant was the quadratic effect of alkali concentration (F value 5.79). The significant terms for the tensile strength surface-reduced quadratic model for PLA/clay composites loaded with Mg(OH)₂-modified K85 rice husks were A, B, AB, AC, BC, B², and C² (see Table 4). Among these, the interactive effect between filler loading and alkali concentration (F value 150.66) was found to be the most significant factor, followed by filler loading (F value 25.86). Quadratic effects of fiber loading and alkali concentration were the least influencing factors with F values of 4.86 and 9.25 respectively.

Meanwhile, A, B, AB, AC, BC, A², and B² are significant terms for the tensile strength surface-reduced quadratic model for PLA/clay composites loaded with NaOH-modified K98 rice husks (see Table 5). Among these, the interactive effect between filler loading and alkali concentration (F value 246.99) was found to be the most significant factor, followed by fiber loading (F value 52.96). The interactive effect between filler loading and fiber loading (F value 9.44) was found to be the least significant influencing factor. A, B, AB, AC, BC, and B² are significant terms for the tensile strength surface-reduced quadratic model for PLA/clay composites loaded with Mg(OH)₂-modified K898 rice husks (see Table 6). Among these, the interactive effect between filler loading and alkali concentration (F value 247.19) was found to be the most significant factor, followed by interactive effect between fiber loading and alkali concentration

Table 4 ANOVA results for response surface-reduced quadratic model of tensile strength of PLA/clay composites loaded with Mg(OH)₂-modified K85 rice husks

Source	Sum of squares	df	Mean square	F value	p value	
Model	173.21	7	24.7449	32.87	1.04E-05	Significant
A-filler loading	19.47	1	19.4688	25.86	0.000658	
B-fiber loading	9.40	1	9.3961	12.48	0.006385	
AB	8.41	1	8.4100	11.17	0.008628	
AC	113.42	1	113.4225	150.67	6.35E-07	
BC	12.43	1	12.4256	16.51	0.00283	
B ²	3.66	1	3.6590	4.86	0.054922	
C ²	6.96	1	6.9618	9.25	0.013995	
Residual	6.78	9	0.7528			
Lack-of-fit	5.03	5	1.0060	2.31	0.219312	Not significant
Pure error	1.75	4	0.4364			
Cor total	179.99	16				
Mean	25.17 ± 0.87			R ²		0.9624
C.V.%	3.45			Adjusted R ²		0.9331
Adequate precision	23.135			Predicted R ²		0.8237

Table 5 ANOVA results for response surface-reduced quadratic model of tensile strength of PLA/clay composites loaded with NaOH-modified K98 rice husks

Source	Sum of squares	df	Mean square	F value	p value	
Model	138.67	7	19.8099	59.67	7.97E-07	Significant
A-filler loading	13.03	1	13.0305	39.25	0.000147	
B-fiber loading	17.58	1	17.5825	52.96	4.68E-05	
AB	3.13	1	3.1329	9.44	0.01331	
AC	81.99	1	81.9930	246.99	7.52E-08	
BC	14.98	1	14.9769	45.12	8.69E-05	
A ²	3.55	1	3.5492	10.69	0.009686	
B ²	4.84	1	4.8400	14.58	0.0041	
Residual	2.99	9	0.3320			
Lack-of-fit	2.02	5	0.4049	1.68	0.317465	Not significant
Pure error	0.96	4	0.2408			
Cor total	141.66	16				
Mean	25.32 ± 0.58			R ²		0.9789
C.V.%	2.28			Adjusted R ²		0.9625
Adequate precision	29.368			Predicted R ²		0.8999

(*F* value 33.51), then filler loading (*F* value 30.42). The quadratic effect of fiber loading (*F* value 15.00) was found to be the least significant influencing factor.

Tables 3–6 also list the statistical data for tensile strengths variance analysis. Coefficient of regression values (*R*²) of 0.9635, 0.9624, 0.9789, and 0.9731 obtained for PLA/clay composites loaded with NaOH-modified K85 rice husks, Mg(OH)₂-modified K85 rice husks, NaOH-modified K98 rice husks, and Mg(OH)₂-modified K98 rice husks, respectively, suggested that the models competently represented the relationship between significant model terms. In fact, this result signalled higher reliability of empirical model data since all the *R*² values were very close to 1 [46, 47]. Such high *R*² values describe the models' fit and the accuracy of the estimated constants [46]. The models

obtained in NaOH-modified rice husks PLA composites achieved more accuracy, as observed to their higher *R*² values (0.9635 and 0.9789) compared to Mg(OH)₂-modified rice husks PLA composites (0.9624 and 0.9731). Similarly, the observation for the adjusted *R*² values for the four models was close to 1. *R*² and adjusted *R*² values were in good agreement, with an approximately 95% confidence level, implying that the experimental and predicted efficiencies were not much different [46, 48]. Additionally, the predicted *R*² values of 0.8293, 0.8237, 0.8999, and 0.9202 for PLA/clay composites loaded with NaOH-modified K85 rice husks, Mg(OH)₂-modified K85 rice husks, NaOH-modified K98 rice husks, and Mg(OH)₂-modified K98 rice husks, respectively, were in reasonable agreement with adjusted *R*² values (respective differences were less than 0.2) [31, 46].

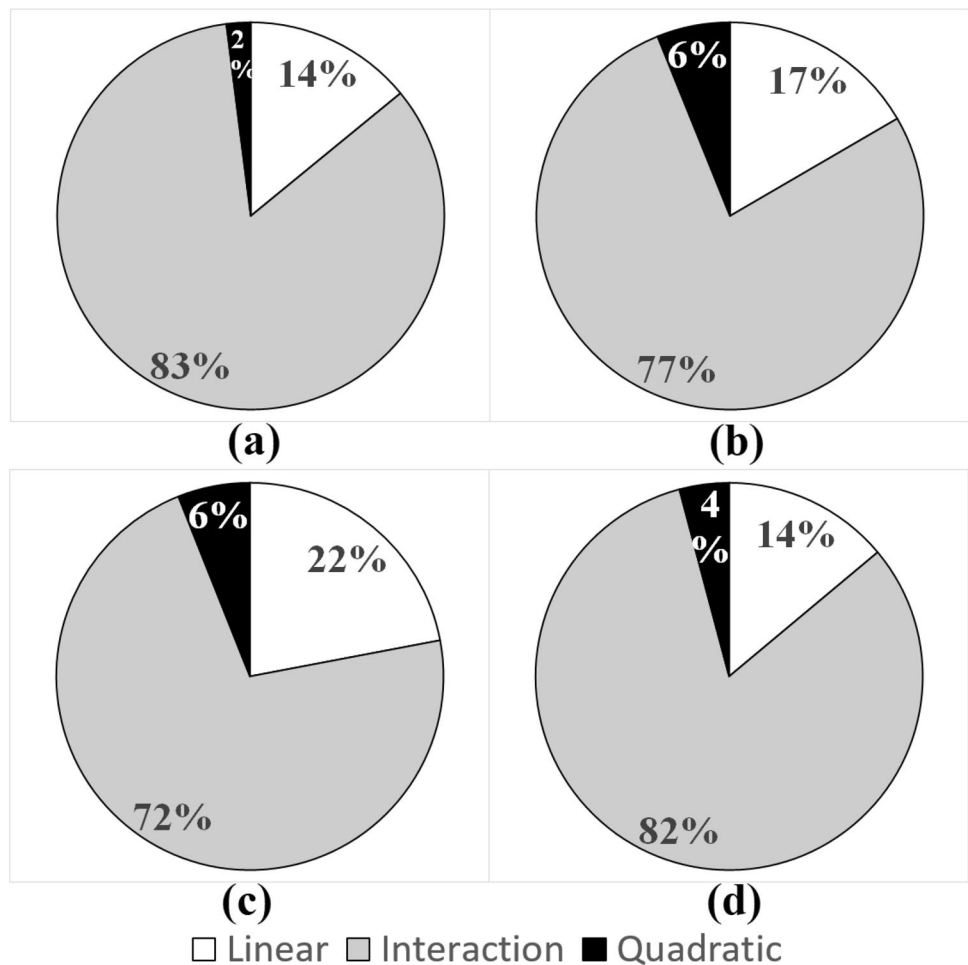
Table 6 ANOVA results for response surface-reduced quadratic model of tensile strength of PLA/clay composites loaded with Mg(OH)₂-modified K98 rice husks

Source	Sum of squares	df	Mean square	F value	p value	
Model	153.69	6	25.6144	60.38	2.81E-07	Significant
A-filler loading	12.90	1	12.9032	30.42	0.000256	
B-fiber loading	8.49	1	8.4872	20.01	0.001192	
AB	6.86	1	6.8644	16.18	0.002428	
AC	104.86	1	104.8576	247.19	2.22E-08	
BC	14.21	1	14.2129	33.51	0.000176	
B ²	6.36	1	6.3614	15.00	0.003096	
Residual	4.24	10	0.4242			
Lack-of-fit	2.34	6	0.3894	0.82	0.60773	Not significant
Pure error	1.91	4	0.4764			
Cor total	157.93	16				
Mean	25.64 ± 0.65			R ²		0.9731
C.V.%	2.60			Adjusted R ²		0.9570
Adequate precision	30.579			Predicted R ²		0.9202

Furthermore, the coefficient of variation (C.V.), which must be lower than 10%, shows precision of the actual and predicted model [25, 39]. The low C.V. values of 2.90%, 3.45%, 2.28%, and 2.60% recorded in models for tensile

strength of PLA/clay composites loaded with NaOH-modified K85 rice husks, Mg(OH)₂-modified K85 rice husks, NaOH-modified K98 rice husks, and Mg(OH)₂-modified K98 rice husks, respectively, show preciseness of the estimate.

Fig. 2 Model term TPCs for PLA/clay composites loaded with (a) NaOH-modified K85 rice husks, (b) Mg(OH)₂-modified K85 rice husks, (c) NaOH-modified K98 rice husks, and (d) Mg(OH)₂-modified K98 rice husks



Adequate precision, which measures the signal to noise ratio, was greater than 4 in each of the models, indicating adequate model discrimination [35]. Adequate precision ratios of 25.888, 23.135, 29.368, and 30.579 obtained in models for tensile strength of PLA/clay composites loaded with NaOH-modified K85 rice husks, Mg(OH)₂-modified K85 rice husks,

NaOH-modified K98 rice husks, and Mg(OH)₂-modified K98 rice husks, respectively, indicated adequate signal and suggested that the respective models can be used to navigate the design space defined by the BBD [42].

The total percentage contributions (TPC) of model terms in each of the reduced quadratic models is

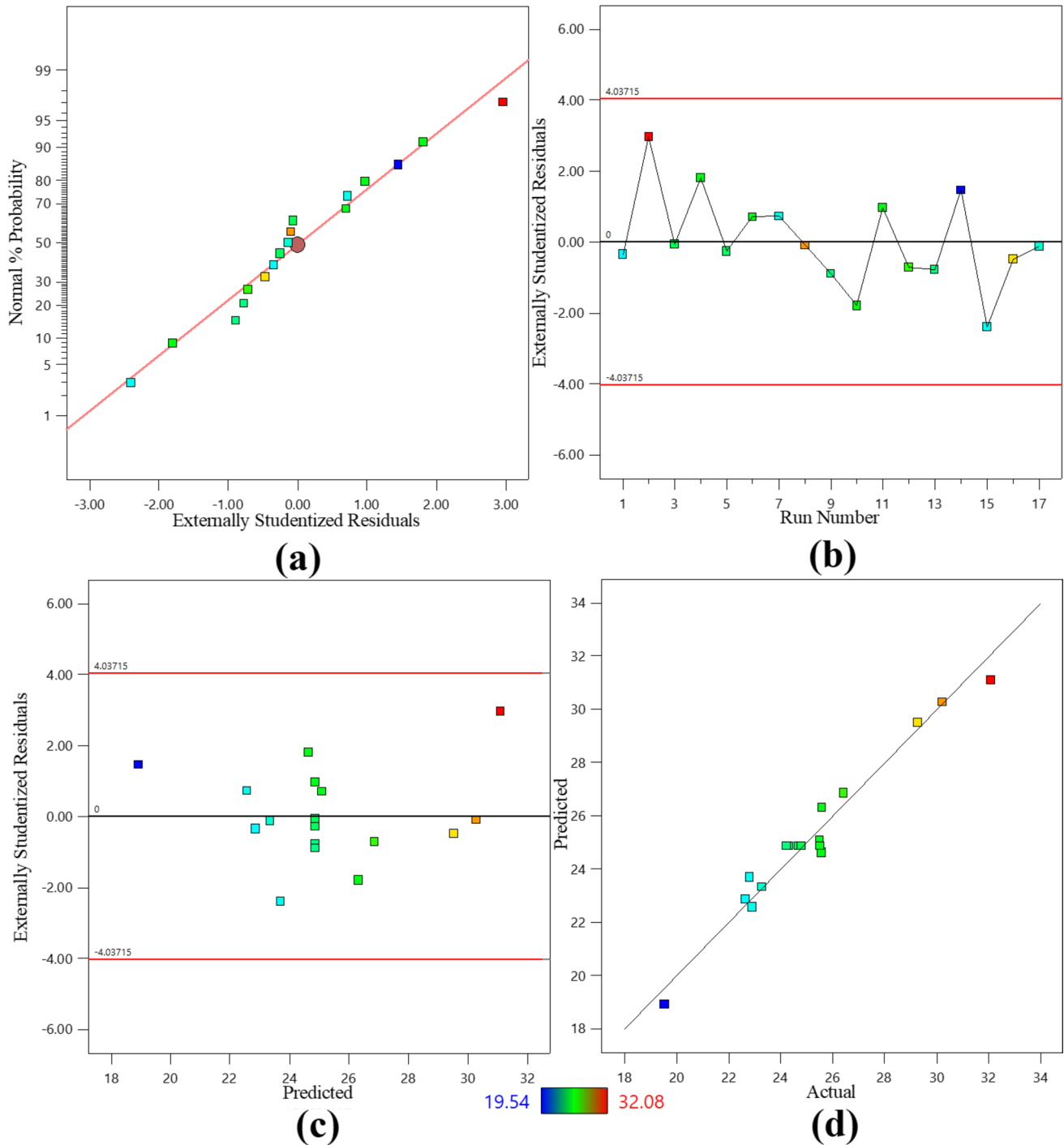


Fig. 3 (a) Normal probability-residual, (b) residual-run, (c) externally studentized residual-predicted response, (d) predicted-actual values following tensile test of PLA/clay/NaOH-modified K85 rice husks

of extreme importance as it shows which of the factors has more effect to the model. In order to obtain the factorial weight or variance part of each factor, the sum of squares (SS) was taken from ANOVA data in

Tables 3 – 6 [36]. As such, TPC of model terms in each of the reduced quadratic models was computed using Eqs. (7) – (9) for the linear, interaction, and quadratic terms respectively [38].

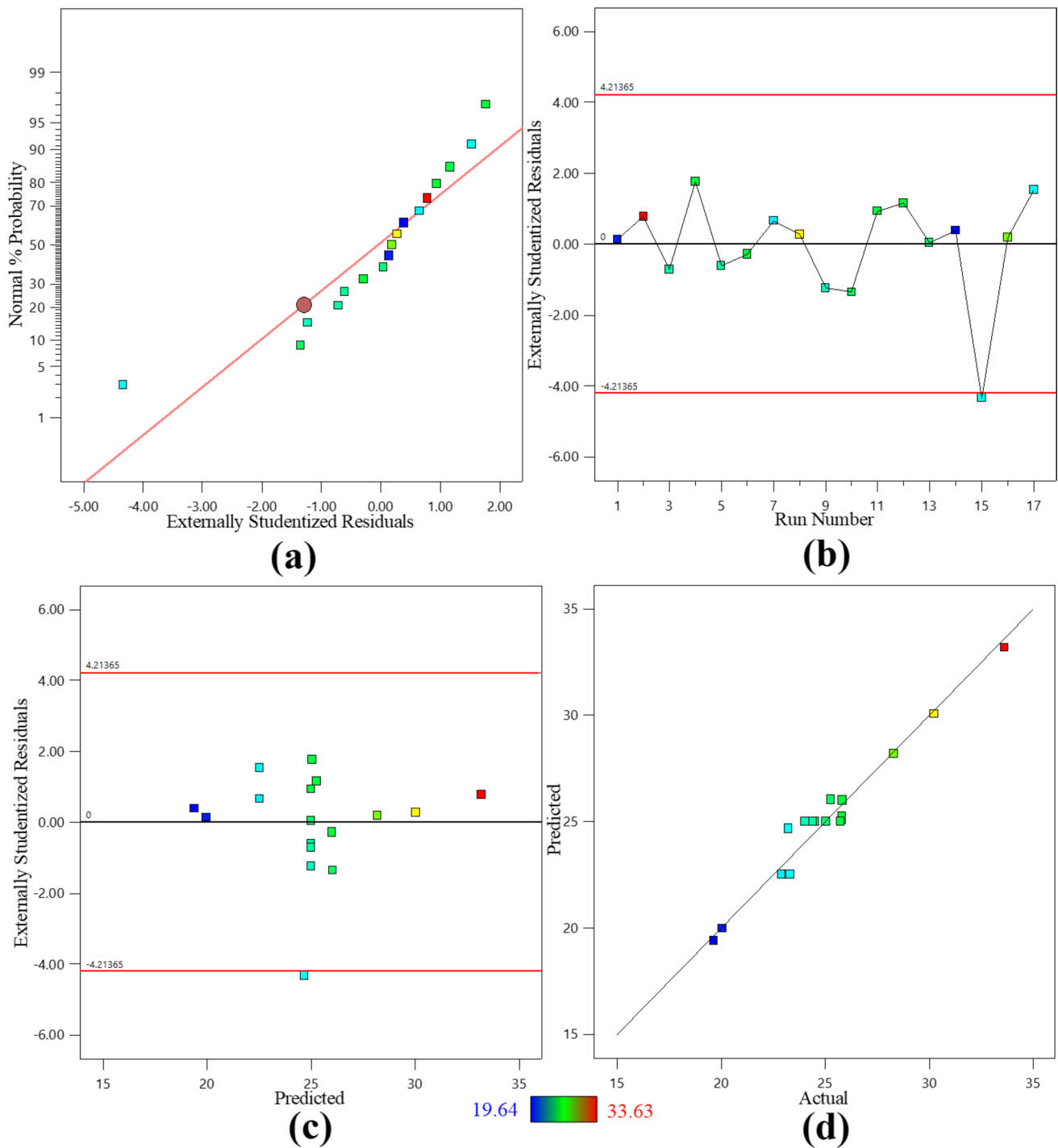


Fig. 4 (a) Normal probability-residual, (b) residual-run (c) externally studentized residual-predicted response, (d) predicted-actual values following tensile test of PLA/clay/Mg(OH)₂-modified K85 rice husks

$$TPC_j = \frac{\sum_{j=1}^k SS_j}{\sum_{i=1}^k \sum_{j=1}^k SS_j + SS_{jj} + SS_{ij}} \times 100 \quad (7)$$

$$TPC_{ij} = \frac{\sum_{i=1}^k \sum_{j=1}^k SS_{ij}}{\sum_{i=1}^k \sum_{j=1}^k SS_j + SS_{jj} + SS_{ij}} \times 100 \quad (8)$$

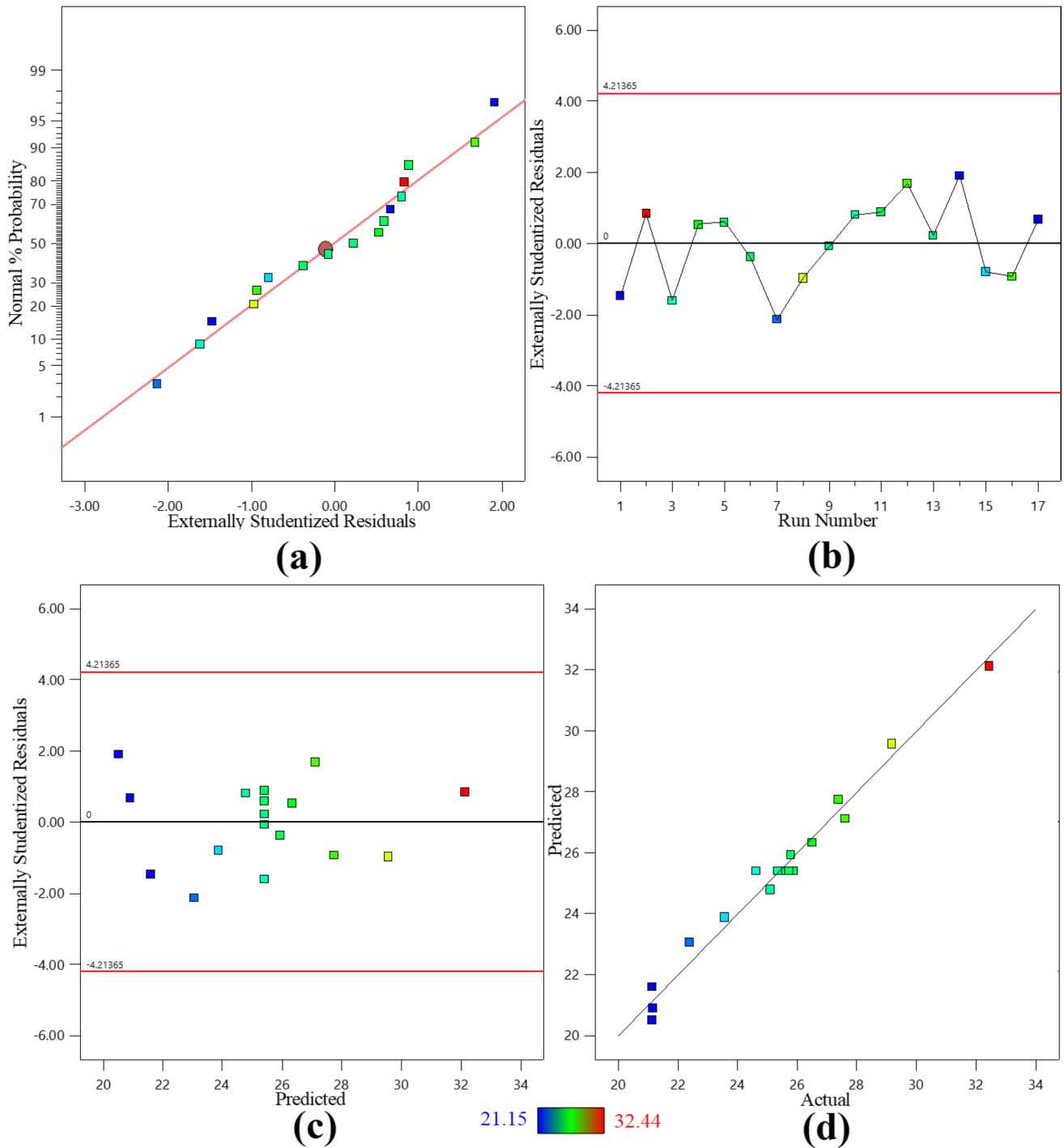


Fig. 5 (a) Normal probability-residual, (b) residual-run, (c) externally studentized residual-predicted response, (d) predicted-actual values following tensile test of PLA/clay/NaOH-modified K98 rice husks

$$TPC_{jj} = \frac{\sum_{i=1}^k \sum_{j=1}^k SS_{ij}}{\sum_{i=1}^k \sum_{j=1}^k SS_j + SS_{jj} + SS_{ij}} \times 100 \quad (9)$$

As shown in Fig. 2, the interaction effect is more predominant than the linear and quadratic effects for tensile

strength of PLA/clay composites, which is consistent with the findings reported in the literature [35]. In fact, the TPC for interaction effects are 83.42%, 77.27%, 71.96%, and 81.94% for PLA/clay composites loaded with NaOH-modified K85 rice husks, Mg(OH)₂-modified K85 rice husks, NaOH-modified K98 rice husks, and

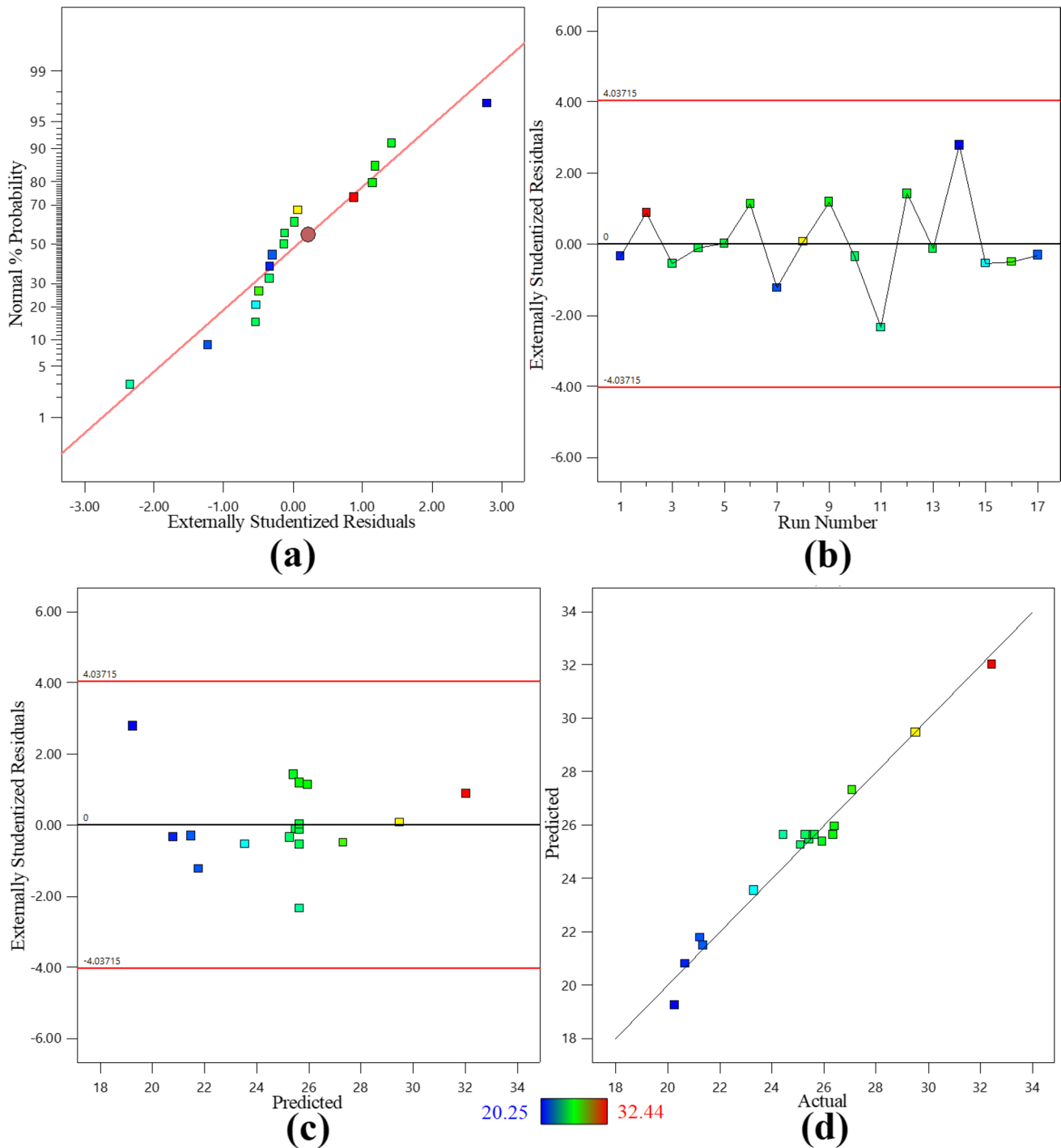


Fig. 6 (a) Normal probability-residual (b) residual-run (c) externally studentized residuals-predicted response (d) predicted-actual values following tensile test of PLA/clay/Mg(OH)₂ modified K98 rice husks

Mg(OH)₂-modified K98 rice husks respectively. Quadratic effects between factors are the least predominant at 2.19%, 6.11%, 6.03%, and 4.14% respectively. Furthermore, for linear effects (basing on sum of squares), clay filler loading can generally be considered the most

important factor, followed by rice husk fiber loading. However, the alkali concentration is less decisive in the reduced quadratic models. This is possibly due to the very minimal concentrations of NaOH and Mg(OH)₂ used in the pre-treatment of rice husk fibers.

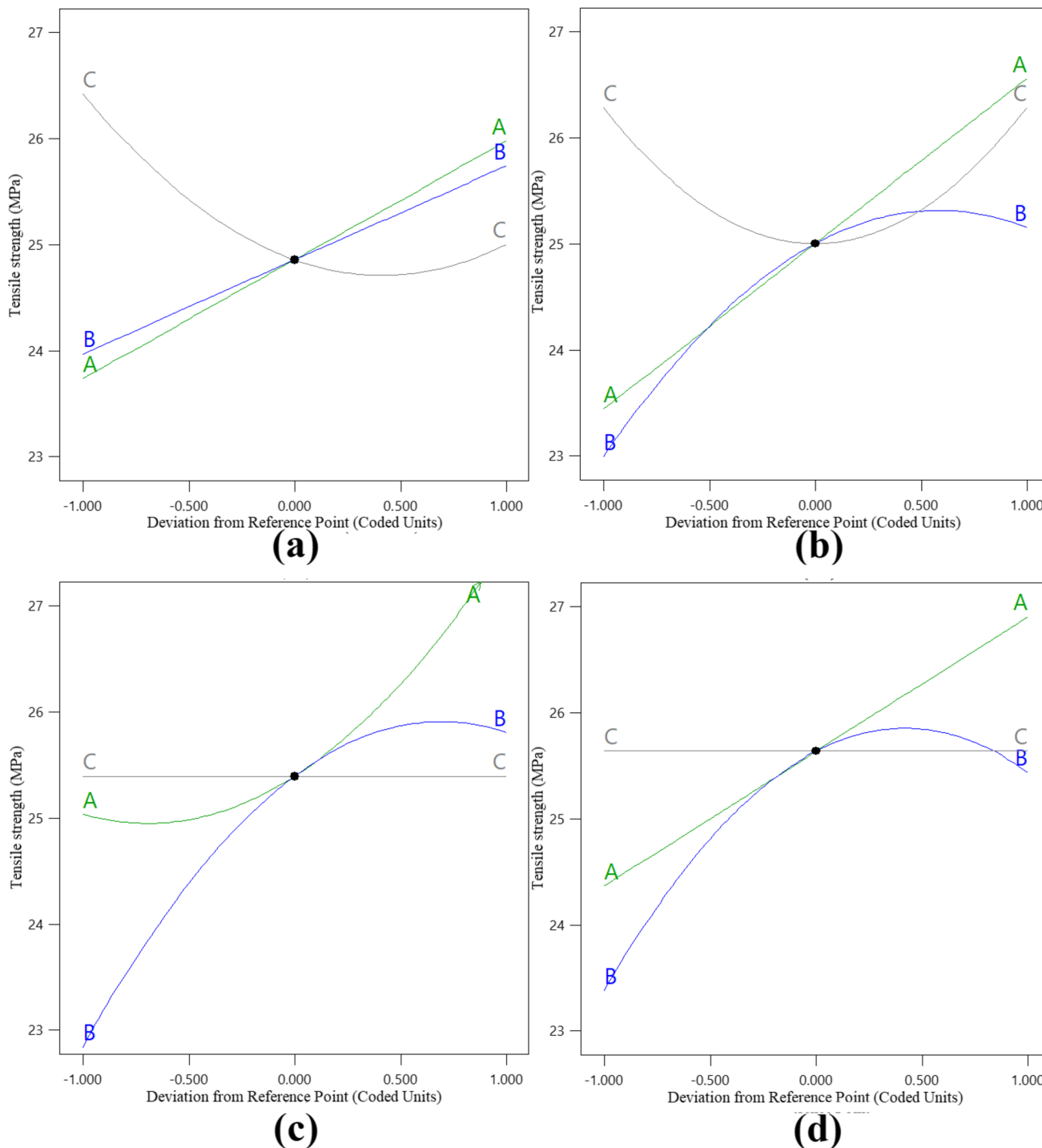
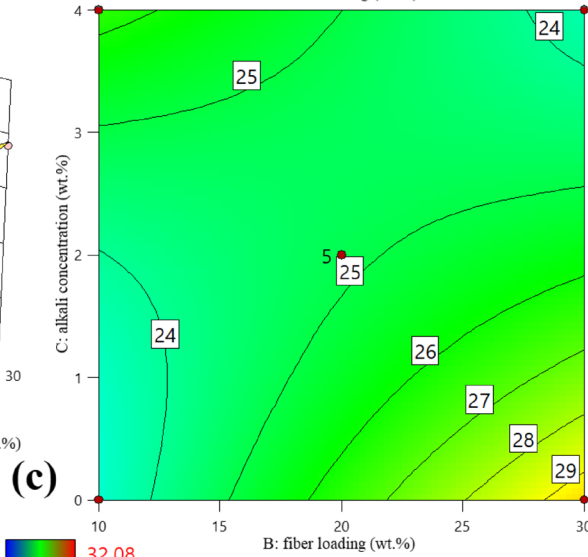
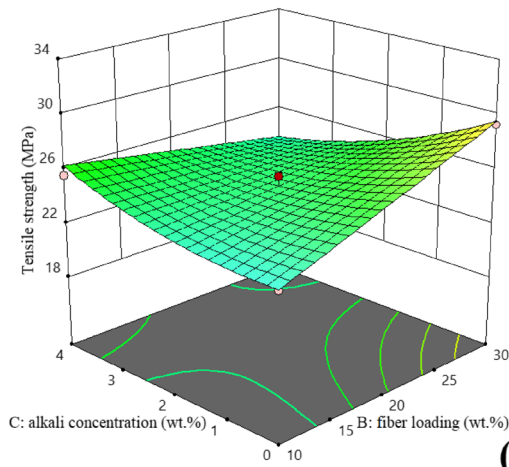
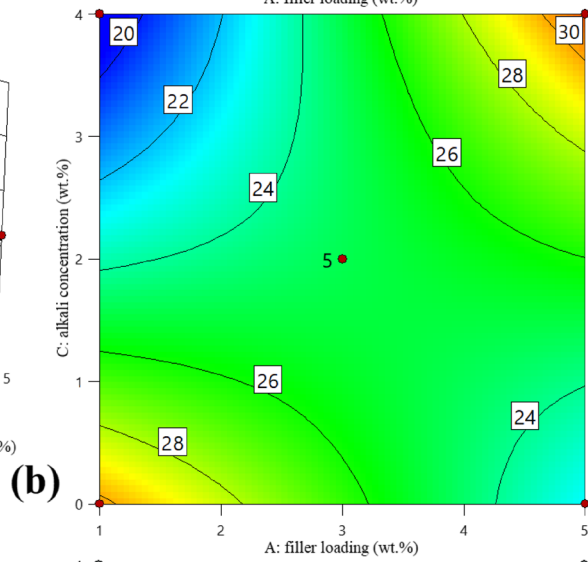
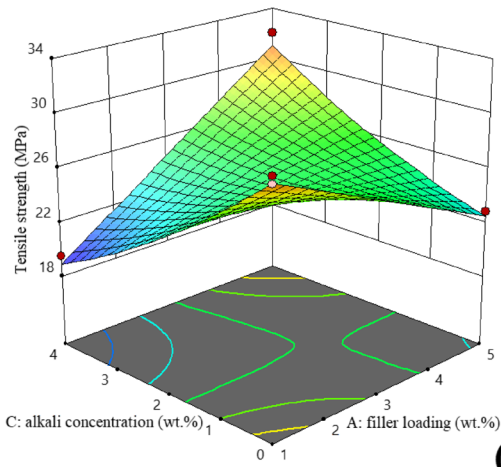
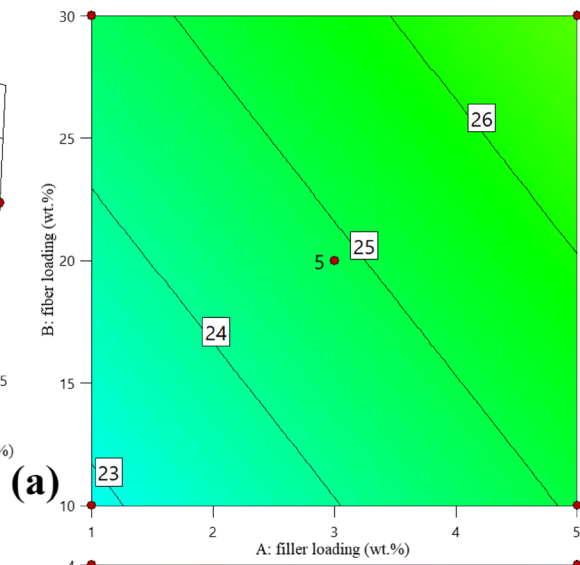
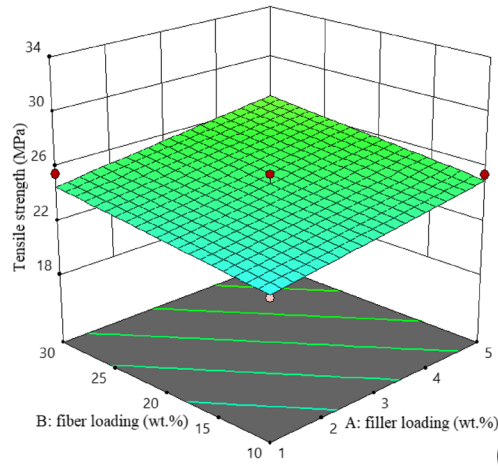


Fig. 7 Main effect perturbation plots for PLA/clay composites loaded with (a) NaOH modified K85 rice husks, (b) Mg(OH)₂ modified K85 rice husks, (c) NaOH modified K98 rice husks and (d) Mg(OH)₂ modified K98 rice husks



◀ **Fig. 8** 3D and 2D plots of (a) fiber loading vs filler loading, (b) alkali concentration vs filler loading, (c) alkali concentration vs fiber loading on tensile strength of PLA/clay/NaOH-modified K85 rice husks.

3.3 Diagnostics and adequacy of residual plots

The adequacy of the fitted models was inspected to verify if the suggested model provided a sufficient approximation of actual systems. To ascertain their validity, normal probability plots of the internally studentized residuals were verified with the assumption of ANOVA values. These were used to obtain the standard deviation between experimental and predicted values. Figures 3a, 4a, 5a, and 6a present the relationship for normal probability distribution and studentized residuals with tensile strengths of PLA/clay composites loaded with NaOH-modified K85 rice husks, Mg(OH)₂-modified K85 rice husks, NaOH-modified K98 rice husks, and Mg(OH)₂-modified K98 rice husks respectively. The residual points showed a curve close to the line that fit model data and the residual values did not display any apparent problem with normality [43, 49]. The correlation between studentized residuals and experimental runs for tensile strength behavior are shown in Figs. 3b, 4b, 5b, and 6b. Almost all the data points fell inconspicuously close to “0,” demonstrating constant variance in experimental observations. For tensile strength of PLA/clay composites developed with Mg(OH)₂-modified K85 rice husks, run 15 (23.23 MPa) recorded the lowest value of residuals (4.332) (see Fig. 4b). This outlier effect explains the why the model for this set of composites had the lowest R^2 value (0.9624). Therefore, no transformation response is required for the experimental designs of this study [50].

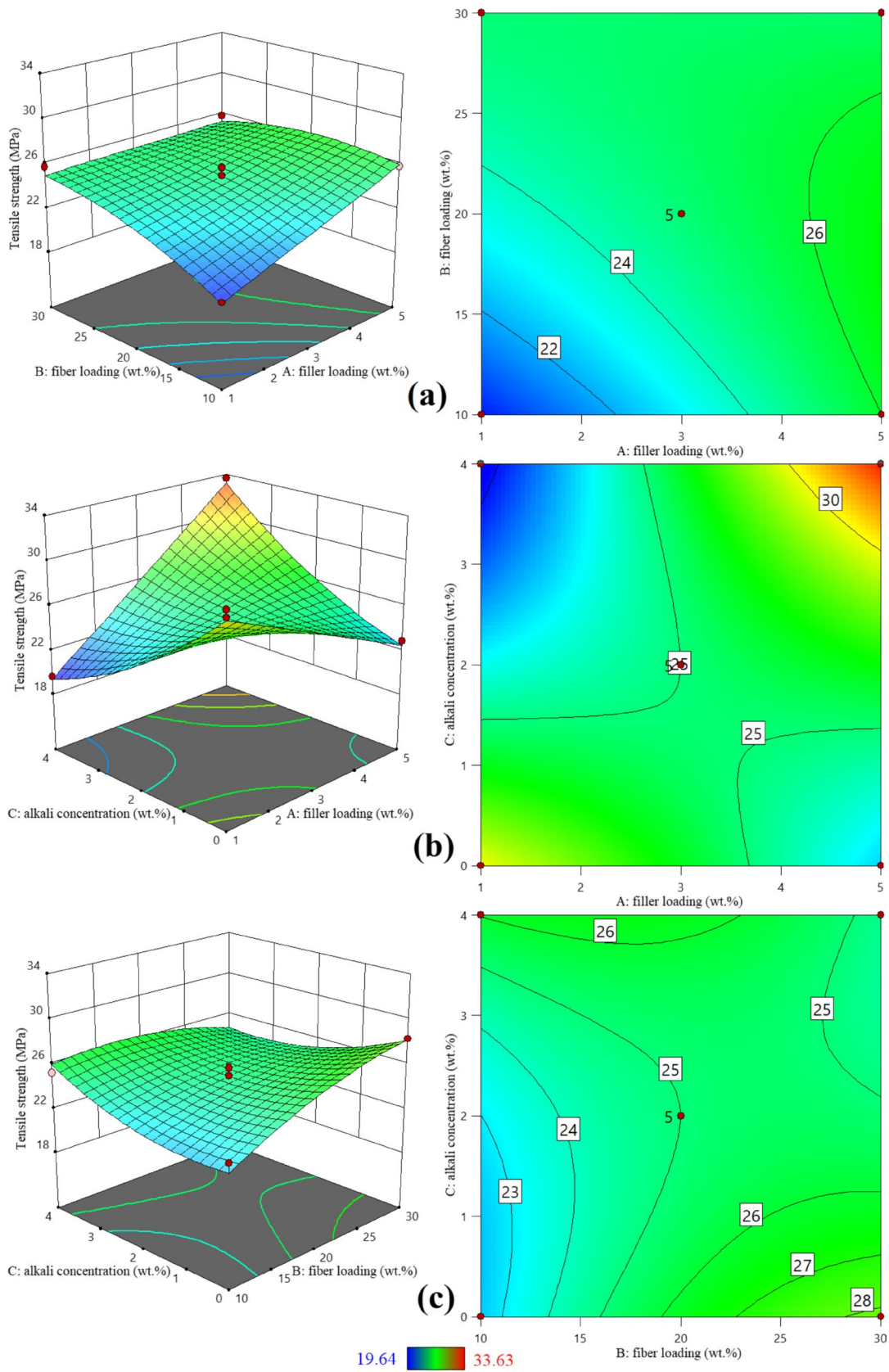
Figures 3c, 4c, 5c, and 6c show the relationship between studentized residuals and predicted tensile strength responses of PLA/clay composites loaded with NaOH-modified K85 rice husks, Mg(OH)₂-modified K85 rice husks, NaOH-modified K98 rice husks, and Mg(OH)₂-modified K98 rice husks respectively. Studentized residuals were randomly scattered in a constant range across plot “0.” These plots did not show any clear pattern, suggesting random distribution of the residuals and hence validating the initial assumption of constant variance [31, 35]. Moreover, all residual data points fell between +4.03715 and −4.03715, proving the adequacy of the quadratic models, especially in relation to the high R^2 values obtained [46]. Linear plots for predicted versus actual values for tensile strengths of the developed composites are shown in Figs. 3d, 4d, 5d, and 6d. All scatter points were correctly distributed close to the 45° line, which suggested high degrees of correlation between the experimental and predicted values. Consequently, the respective developed response surface models can be used to adequately represent the functional relationships between the experimental factors and tensile strengths of fiber-reinforced PLA composites.

Perturbation plots were used to provide correlations for process parameters at the respective center point on the tensile strengths (see Fig. 7). These plots provided a better understanding of the results. Particularly, a perturbation plot demonstrates the response of a particular factor in movement from a chosen center/reference point while other factors remain fixed [51]. In this study, the reference point was set in the center of the design space, which was the zero-coded level of each factor (3 wt.% filler loading, 20 wt.% fiber loading and 2 wt.% alkali concentration). It was seen that tensile strength of PLA/clay composites developed with NaOH-modified K85 rice husks increased with increases in filler loading and fiber loading (see Fig. 7a). This is because fillers and fibers provide reinforcement to PLA matrix and transfer stress from one fiber/filler to the next, thereby enabling an even distribution of the stress throughout the developed composite [52]. For Mg(OH)₂-modified rice husks PLA/clay composites, increase in fiber loading past the center point (20 wt.%) led to a reduction in tensile strength (see Fig. 7b). The curvature for alkali concentration is much sharper than the other curves, indicating that the tensile strength of this set of PLA/clay composites was more sensitive to alkali concentration (see Fig. 7a and b). The high sensitivity is due to the quadratic effect of alkali concentration in these particular models (see Eqs. 3 and 4). At low levels of alkali concentration, tensile strength was high but reduced to a minimum value at the center point, before increasing again. It should be noted, however, that the increase after the center point (2 wt.%) was sluggish compared to that before the center point.

For PLA/clay composites developed with K98 rice husks, tensile strengths increased with increases in filler loading and fiber loading (see Fig. 7c and d). The curvature for fiber loading was much sharper than the other curves, indicating that the tensile strength of this set of PLA/clay composites was more sensitive to fiber loading, followed by filler loading as confirmed by the quadratic effect of fiber loading in these particular models (see Eqs. 5 and 6). It should be noted, however, that the increase in fiber loading after the center point (20 wt.%) was sluggish compared to that before the center point. Tensile strengths of composites loaded with more than 20 wt.% fiber are likely to drop because the amount of PLA matrix would be insufficient to wet out the fiber and fully transfer the stress effectively at such high fiber loadings [52]. Meanwhile, alkali concentration had no striking effect on tensile strengths of PLA/clay composites developed with K98 rice husks.

3.4 Response surface contour plots

The three-dimensional (3D) response and two-dimensional (2D) contour effects of the process factors on tensile strength behavior of PLA/clay composites loaded with



◀ **Fig. 9** 3D and 2D plots of (a) fiber loading vs filler loading, (b) alkali concentration vs filler loading, (c) alkali concentration vs fiber loading on tensile strength of PLA/clay/Mg(OH)₂-modified K85 rice husks.

NaOH-modified K85 rice husks are shown in Fig. 8. Figure 8a shows the interaction effect of rice husk fiber loading and clay filler loading on tensile strength. It can be ascertained from the silhouette view of all process parameters in the 3D surface plot that an increase in filler loading led to increasing tensile strengths by up to 12.68% at maximum filler loading. In addition, an increase in fiber loading also increased composites tensile strength due to better interlocking between the fiber/filler and PLA matrix [19, 43]. Similar findings were reported by King et al. [53]. This effect is clearly seen in the 2D contour plot, where the tensile strength was the lowest at 10 wt.% fiber loading and increased steadily up to 25.58 MPa and 26.43 MPa at 30 wt.% fiber loading, depending on the alkali concentration ratio. Jandas et al. [24] reported that increased fiber loadings coupled with increased clay filler loadings increase tensile strengths.

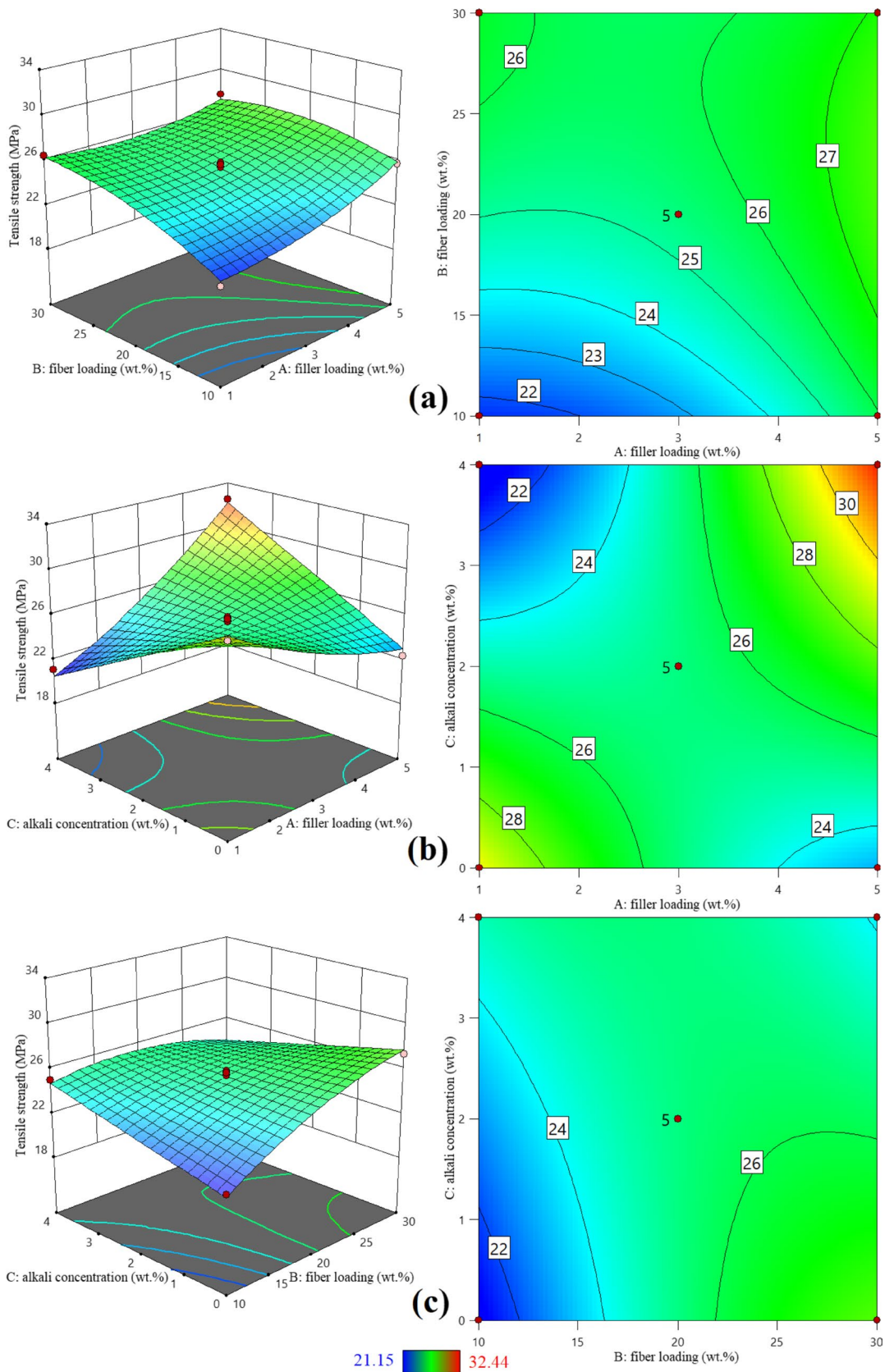
Figure 8b shows a silhouette view for all alkali concentration and clay filler loading process parameters and tensile strength. The 3D response surface plot confirms that tensile strength of PLA/clay composites developed with raw K85 rice husks decreases with increases in filler loading from 30.22 to 22.91 MPa. An opposite trend is realised when the husks are modified at 4 wt.% NaOH concentrations. Tensile strengths at 4 wt.% NaOH concentrations increase tensile strength by 64.18% due to better interaction, compatibility, and adhesion between both clay and NaOH-modified K85 rice husks to the PLA matrix [27]. At low filler levels, tensile strength reduced due to alkali modification of K85 rice husks while at the highest filler loading conditions, tensile strength of the developed composites increased with alkali modification of K85 rice husks. The 2D contour plot illustrates that tensile strength value was the highest at 5 wt.% filler loading (32.08 MPa) when K85 rice husks were modified with 4 wt.% concentration of NaOH, increasing by 40% from the value obtained when raw K85 rice husks were used. The realisation is that when low filler amounts are used, it is not necessary to modify the K85 rice husks while when higher filler amounts are to be used, higher concentrations of NaOH are required to modify K85 rice husks so as to enhance compatibility with PLA matrix.

The interaction effect for the response surface plot of NaOH concentration versus fiber loading on tensile strength of PLA/clay composites developed with K85 rice husks is represented in Fig. 8c. Tensile strength increased from 23.27 MPa with increases in raw K85 rice husk fiber loading to a maximum tensile strength of 29.29 MPa as viewed in the 2D plot of Fig. 8c. The increase in tensile strength at these conditions was also reported by Ibrahim et al. [54] who

incorporated 10–30% kenaf fibers into PLA matrix. They reported increasing tensile strengths of the composites with increasing fiber loading. An opposite trend is seen in the 3D response surface plot at 4 wt.% NaOH-modified K85 rice husks as tensile strength reduced by 10.90% to 22.80 MPa. Similar results were obtained by Hassan et al. [35]. This result is in disagreement with Ng et al. [55] who proposed that high alkali concentrations (5 wt.%) and high fiber loadings (30 wt.%) improve biocomposites' tensile strengths due to low hemicellulose levels. Meanwhile, at low fiber loadings, increase in alkali concentration increased tensile strength of the composites while at higher fiber loadings, increase in alkali concentration decreased tensile strengths from 29.29 to 22.80 MPa. Fig. 8:3D and 2D plots of a fiber loading vs filler loading, b alkali concentration vs filler loading, c alkali concentration vs fiber loading on tensile strength of PLA/clay/NaOH-modified K85 rice husks. Fig. 8:3D and 2D plots of a fiber loading vs filler loading, b alkali concentration vs filler loading, c alkali concentration vs fiber loading on tensile strength of PLA/clay/NaOH-modified K85 rice husks.

Figure 9 shows the three-dimensional (3D) response and two-dimensional (2D) contour effects of the process factors on tensile strength behavior of PLA/clay composites loaded with Mg(OH)₂-modified K85 rice husks. Figure 9a shows the interaction effect of rice husk fiber loading and clay filler loading on tensile strength. From the silhouette view of all process parameters in the 3D surface plot, at low fiber loading ratios (10 wt.%), an increase in filler loading increased the tensile strengths from 20.05 to 25.85 MPa. At high fiber loading ratios, increasing filler loading had no effect on tensile strength as it remained constant at 25.82 MPa. In addition, as clearly seen in the 2D contour plot, tensile strengths did not change much with increase in fiber loading at the highest clay filling ratio (5 wt.%). Meanwhile, at the lowest clay filler ratio, an increase in fiber loading increased composites' tensile strength due to reduced micro-voids, enhanced uniform dispersion and adhesion between the fiber-filler-PLA interface [56].

Figure 9b shows a silhouette view for all Mg(OH)₂ concentration and clay filler loading process parameters and tensile strength. The 3D response surface plot confirms that tensile strength of PLA/clay composites developed with raw K85 rice husks decreases with increases in filler loading by 24.19%. Similar findings were reported by Ramesh et al. [56] who reported that increase in clay filler loading diminished the tensile strength of kenaf/aloevera fiber-reinforced PLA composites by having micro-voids and agglomerations formations, which reduced fiber-PLA bonding and load transfer capacity. Similar to the trend in tensile strength of PLA/clay



◀ **Fig. 10** 3D and 2D plots of (a) fiber loading vs filler loading, (b) alkali concentration vs filler loading, (c) alkali concentration vs fiber loading on tensile strength of PLA/clay/NaOH-modified K98 rice husks.

composites developed with 4 wt.% NaOH-modified K85 rice husks, tensile strength of PLA/clay composites developed with 4 wt.% Mg(OH)₂-modified K85 rice husks, increased by 71.23% with increase in clay filler loading. Additionally, at low filler levels, tensile strength decreased with Mg(OH)₂ modification of K85 rice husks while at the 5 wt.% filler loading conditions, tensile strength of the developed composites increased from 22.91 to 33.63 MPa.

The interaction effect for the response surface plot of Mg(OH)₂ concentration versus fiber loading on tensile strength of PLA/clay composites developed with K85 rice husks is represented in Fig. 9c. The 2D plot in Fig. 9c shows that tensile strength increased from 23.27 MPa with increases in raw K85 rice husk fiber loading to a maximum tensile strength of 28.32 MPa. At 4 wt.% Mg(OH)₂ modification, tensile strength reduced from 25.29 to 23.23 MPa. The effect of increasing alkali concentration on tensile strength at the least and highest filler loadings is similar to that obtained in PLA/clay composites developed with NaOH-modified K85 rice husks. Fig. 9:3D and 2D plots of a fiber loading vs filler loading, b alkali concentration vs filler loading, c alkali concentration vs fiber loading on tensile strength of PLA/clay/Mg(OH)₂-modified K85 rice husks. Fig. 9:3D and 2D plots of a fiber loading vs filler loading, b alkali concentration vs filler loading, c alkali concentration vs fiber loading on tensile strength of PLA/clay/Mg(OH)₂-modified K85 rice husks. Fig. 9:3D and 2D plots of a fiber loading vs filler loading, b alkali concentration vs filler loading, c alkali concentration vs fiber loading on tensile strength of PLA/clay/Mg(OH)₂-modified K85 rice husks.

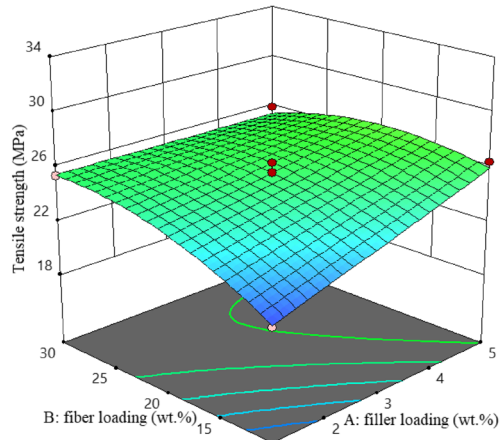
Figure 10 shows the three-dimensional (3D) response and two-dimensional (2D) contour effects of the process factors on tensile strength behavior of PLA/clay composites loaded with NaOH-modified K98 rice husks. Interaction effects between fiber loading and filler loading on tensile strength are shown in Fig. 10a. As seen in the 3D surface plot, at low fiber loading ratios (10 wt.%), an increase in filler loading increased the tensile strengths from 21.15 to 25.79 MPa. This is because at low fiber loadings, clay played a significant role in the adsorption of hydroxyl groups on the rice husks surface and chemical bonds in PLA [57]. Similarly, at high fiber loading ratios, increasing filler loading increased tensile strength but to a minimal change (4.15%). Tensile strengths increased by 7.06% with increase in fiber loading at 5 wt.% filler ratio, while at the lowest clay filler ratio, an increase in fiber loading increased composites' tensile strength from 21.15 to 26.51 MPa. Similar findings were reported by Ramesh et al. [58] who concluded that 1% clay filler addition in 30 wt.% kenaf fiber-reinforced PLA

composites demonstrated the highest tensile strength compared to other formulations.

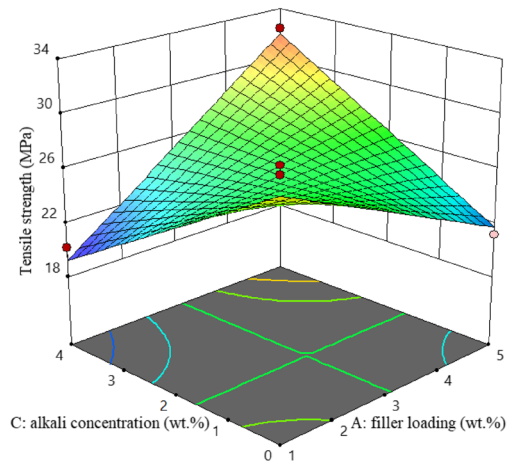
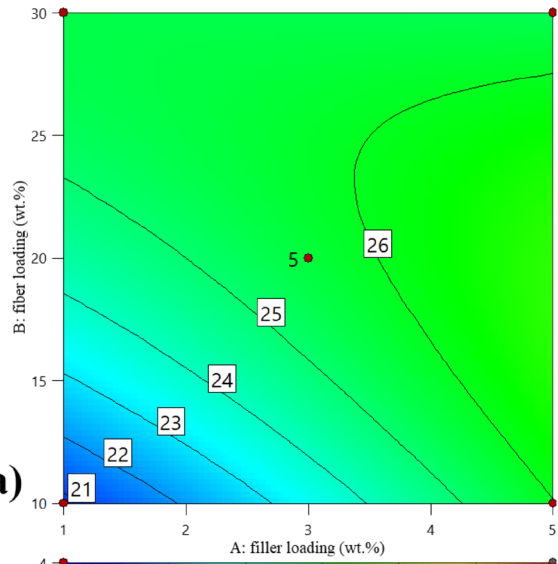
Figure 10b shows a silhouette view for all NaOH concentration and filler loading process parameters and tensile strength. The 3D response surface plot confirms that tensile strength of PLA/clay composites developed with raw K98 rice husks decreases with increases in filler loading from 29.19 to 22.37 MPa. Tensile strength of PLA/clay composites developed with 4 wt.% NaOH-modified K98 rice husks, increased from 21.15 MPa by 53.38% with increase in clay filler loading. Additionally, at low clay filler levels, tensile strength decreased with NaOH modification of K98 rice husks from 29.19 to 21.15 MPa while at 5 wt.% clay filler loading conditions, tensile strength of the developed composites increased by 45.02%. The decrease in tensile strength at low clay filler levels could likely be due to the plasticizing effect, which happened because NaOH has lower molecular weights than PLA matrix [15].

Figure 10c presents the interaction effect for the response surface plot of NaOH concentration versus fiber loading on tensile strength of PLA/clay composites developed with K98 rice husks. From the 3D response surface plot, it is clear that tensile strength increased from 21.17 MPa with increases in raw K98 rice husk fiber loading to a maximum tensile strength of 27.38 MPa. At 4 wt.% NaOH modification, tensile strength reduced by 6.10% to 23.56 MPa. The effect of increasing NaOH concentration on tensile strength and the 1 wt.% and 5 wt.% clay filler loadings is similar to that obtained in PLA/clay composites developed with NaOH-modified K85 rice husks. Fig. 10:3D and 2D plots of a fiber loading vs filler loading, b alkali concentration vs filler loading, c alkali concentration vs fiber loading on tensile strength of PLA/clay/NaOH-modified K98 rice husks. Fig. 10:3D and 2D plots of a fiber loading vs filler loading, b alkali concentration vs filler loading, c alkali concentration vs fiber loading on tensile strength of PLA/clay/NaOH-modified K98 rice husks. Fig. 10:3D and 2D plots of a fiber loading vs filler loading, b alkali concentration vs filler loading, c alkali concentration vs fiber loading on tensile strength of PLA/clay/NaOH-modified K98 rice husks.

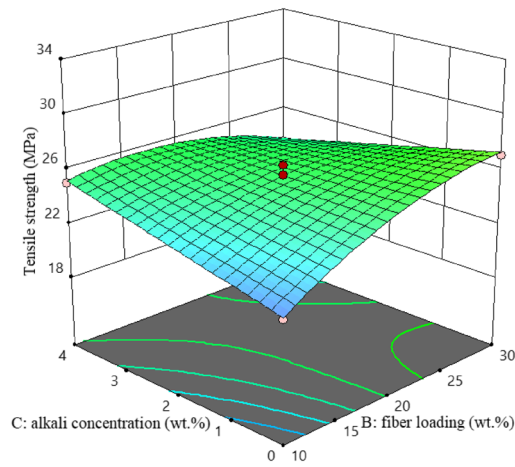
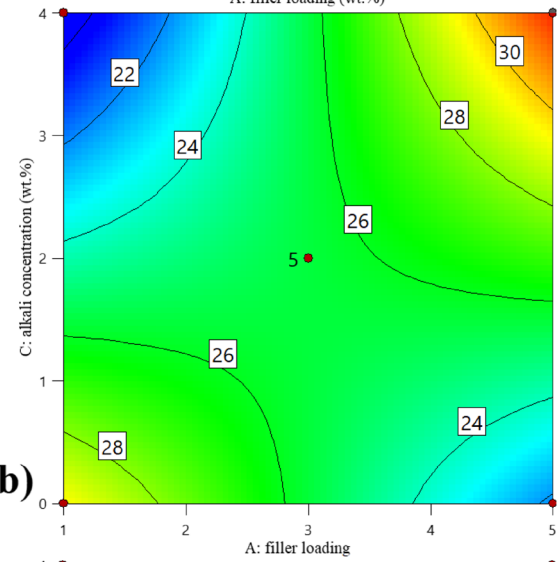
Figure 11 shows the three-dimensional (3D) response and two-dimensional (2D) contour effects of the process factors on tensile strength behavior of PLA/clay composites loaded with Mg(OH)₂-modified K98 rice husks. The interaction between fiber loading and filler loading on tensile strength is shown in Fig. 11a. As seen in the 3D surface plot, at low fiber loading ratios (10 wt.%), an increase in filler loading increased the tensile strengths by 27.83% while at high fiber loading ratios (30 wt.%), increasing clay filler loading increased tensile strength by only 2.01% to 29.54 MPa. At 5 wt.% filler ratio, tensile strengths decreased slightly from 26.41 to 25.94 MPa with increase in fiber loading, while



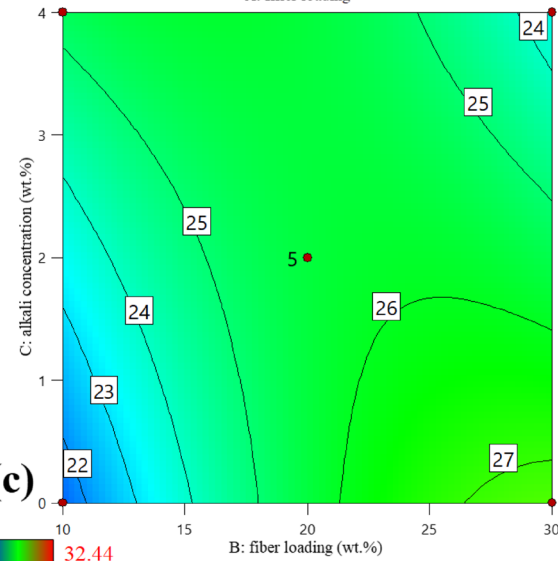
(a)



(b)



(c)



20.25 32.44

◀ **Fig. 11** 3D and 2D plots of (a) fiber loading vs filler loading (b) alkali concentration vs filler loading, (c) alkali concentration vs fiber loading on tensile strength of PLA/clay/Mg(OH)₂-modified K98 rice husks.

at the lowest clay filler ratio (1 wt.%), an increase in fiber loading increased composites' tensile strength from 20.66 to 25.43 MPa. Decreased tensile strength at 5 wt.% clay filler loading is because increased clay amounts inclusion in rice husk fiber-reinforced composites reduces the intercalation level, owing to poor interaction between PLA matrix and raw rice husk fibers [57, 59].

Figure 11b shows a silhouette view for all Mg(OH)₂ concentration and filler loading process parameters and tensile strength. The 3D response surface plot presents that tensile

strength of PLA/clay composites developed with raw K98 rice husks decreases with increases in filler loading from 29.52 to 21.23 MPa. This 27.78% reduction is clearly shown in the 2D contour plot. Tensile strength of PLA/clay composites developed with 4 wt.% Mg(OH)₂-modified K98 rice husks increased from 20.25 to 32.44 MPa, which is a 60.20% with increase in clay filler loading. At low clay filler loading levels (1 wt.%), tensile strength decreased with Mg(OH)₂ modification of K98 rice husks from 29.52 to 20.25 MPa while at 5 wt.% clay filler loading levels, tensile strength of the developed composites increased by 52.80% from 21.23 to 32.44 MPa when raw K98 rice husks were modified with 4 wt.%.

The interaction effect for the response surface plot between Mg(OH)₂ concentration and fiber loading on tensile

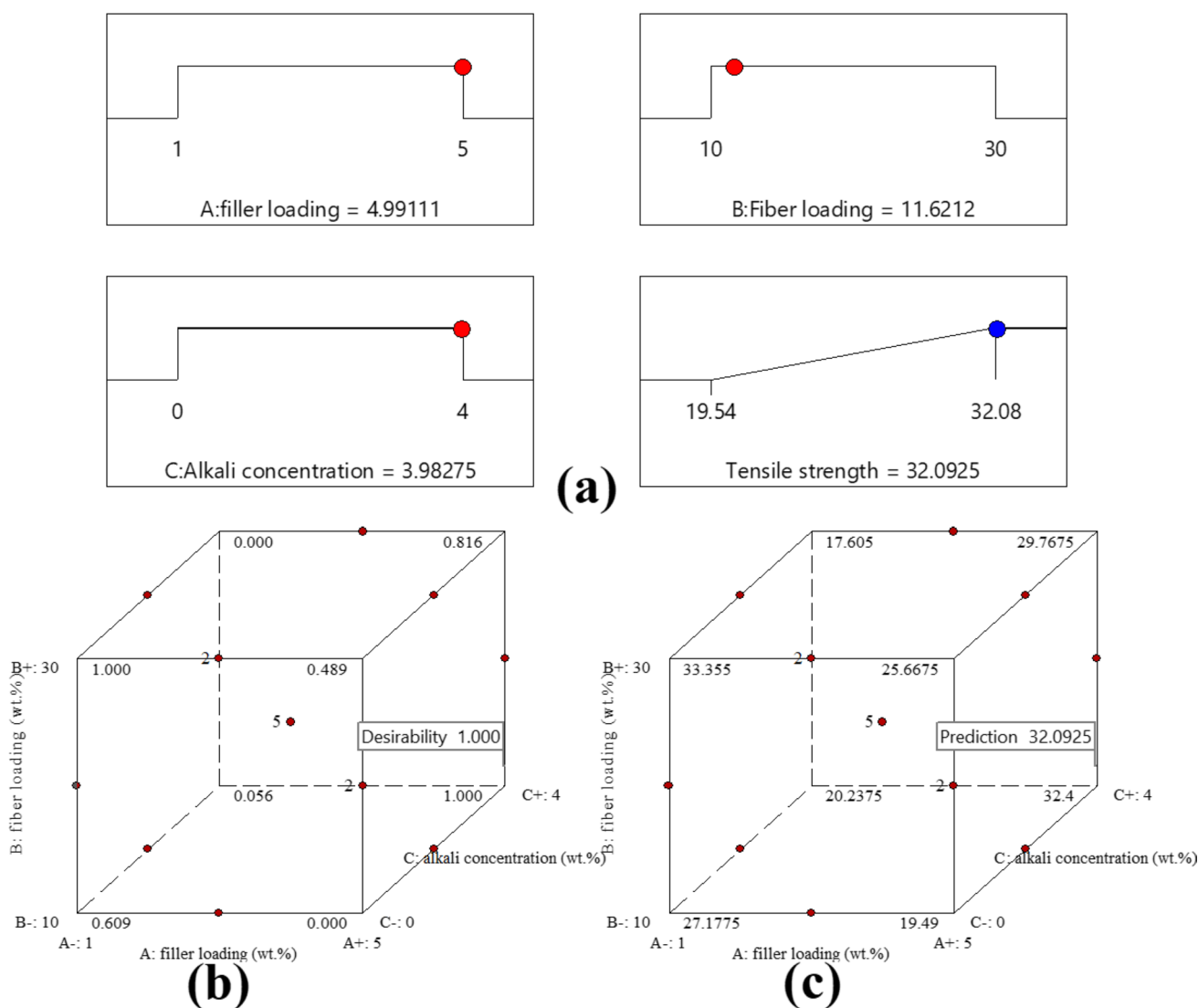


Fig. 12 Typical (a) ramp, (b) desirability cube, (c) tensile strength cube for optimization of filler loading, fiber loading, and alkali modification for PLA/clay/NaOH-modified K85 rice husks

strength of PLA/clay composites developed with K98 rice husks is shown in Fig. 11c. From the 3D response surface plot, it is clear that tensile strength increased by 25.89% from 21.35 to 27.09 MPa with increases in raw K98 rice husk fiber loading while at 4 wt.% NaOH modification of K98 rice husks, a 7.17% reduction in tensile strength from 25.10 MPa was noted. Decreasing tensile strengths at 4 wt.% $\text{Mg}(\text{OH})_2$ concentration are possibly because this concentration is high and unevenly distributed on the husks' surface, which may have aggregated into large particles and caused ununiform cross-link density between the husks and PLA matrix [60]. Meanwhile, at low K98 rice husk fiber loadings (10 wt.%), alkali concentration increased tensile strength of the developed fiber-reinforced PLA composites from 21.35 to 25.10 MPa while at higher fiber loadings (30 wt.%), alkali concentration decreased tensile strengths from 27.09

to 23.30 MPa. Fig. 11:3D and 2D plots of a fiber loading vs filler loading, b alkali concentration vs filler loading, c alkali concentration vs fiber loading on tensile strength of PLA/clay/ $\text{Mg}(\text{OH})_2$ -modified K98 rice husks. Fig. 11:3D and 2D plots of a fiber loading vs filler loading, b alkali concentration vs filler loading, c alkali concentration vs fiber loading on tensile strength of PLA/clay/ $\text{Mg}(\text{OH})_2$ -modified K98 rice husks. Figs. 8, 10, 11.

3.5 Process optimization

After model simulation using the numerical optimization method of the Design-Expert software, optimum conditions

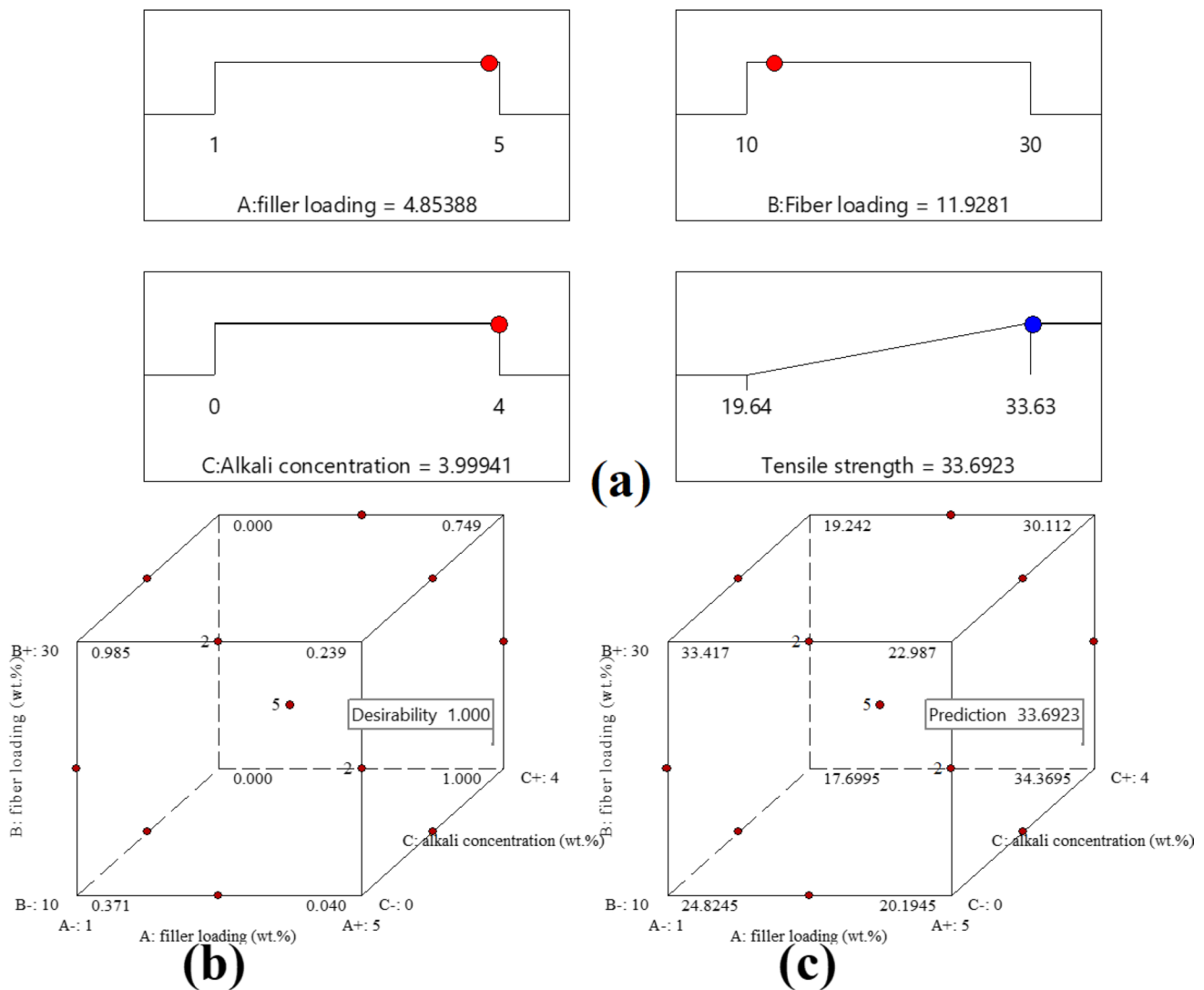


Fig. 13 Typical (a) ramp, (b) desirability cube, (c) tensile strength cube for optimization of filler loading, fiber loading, and alkali modification for PLA/clay/ $\text{Mg}(\text{OH})_2$ -modified K85 rice husks

were suggested for maximizing the tensile strength for each set of fiber-reinforced PLA composites [25, 35, 61–64].

Figures 12, 13, 14 and 15 show the typical ramps, desirability cubes, and tensile strength cubes for optimization of filler loading, fiber loading, and alkali modification for the developed composites. As observed from Figs. 8 – 11, maximum tensile strengths were obtained when filler loading, fiber loading, and alkali concentration were kept in range. Meanwhile, in order to optimize tensile strength in each set of developed composites, individual maximums were targeted. The target goals were between 19.54 – 30.08 MPa, 19.64 – 33.63 MPa, 21.15 – 32.44 MPa, and 20.25 – 32.44 MPa for PLA/clay composites loaded with NaOH-modified K85 rice husks, Mg(OH)₂-modified K85 rice husks, NaOH-modified K98 rice husks, and Mg(OH)₂-modified K98 rice

husks respectively. The typical ramp and cube for optimization of tensile strength of PLA/clay composites loaded with NaOH-modified K85 rice husks are shown in Fig. 12a. Optimal operating conditions for tensile strength were a filler loading of 4.99111 wt.%, fiber loading of 11.6212 wt.%, and a NaOH concentration 3.98275 wt.%. According to the BBD results, the predicted tensile strength was 32.0925 MPa. Meanwhile, a maximum tensile strength of 33.6923 MPa was predicted for PLA/clay composites loaded with Mg(OH)₂-modified K85 rice husks at a filler loading of 4.85388 wt.%, fiber loading of 11.9281 wt.%, and a NaOH concentration 3.99941 wt.% (see Fig. 13a). The optimization conditions for PLA composites developed with modified K98 rice husks were suggested as follows: filler loading (1.02221 wt.% and 4.9653 wt.%), fiber loading (29.3413 wt.% and 12.2886

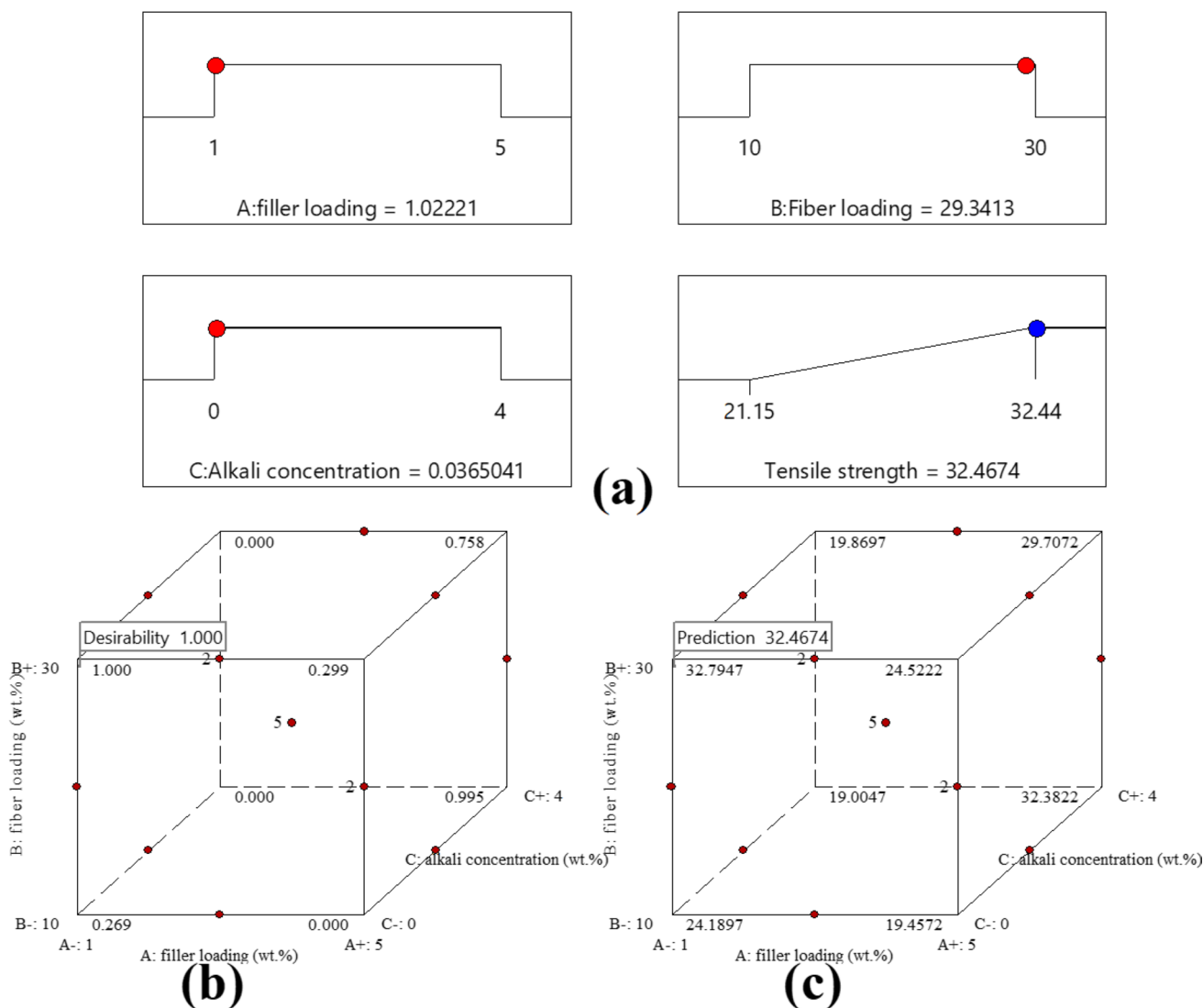


Fig. 14 Typical (a) ramp, (b) desirability cube, (c) tensile strength cube for optimization of filler loading, fiber loading, and alkali modification for PLA/clay/NaOH-modified K98 rice husks

wt.%) and alkali concentration (0.0365041 wt.% and 3.97191 wt.%) for PLA/clay composites developed with NaOH-modified K98 rice husks and $\text{Mg}(\text{OH})_2$ -modified K98 rice husks respectively (see Figs. 14a and 15a). If composites were to be developed at these conditions, the tensile strengths as predicted by the respective developed models are 32.4674 MPa and 32.7468 MPa respectively.

To generate optimum conditions for the tensile strengths of respective composites' sets, the desirability function is employed and values close to 1 are most effective parameters with respect to response factors [25, 46, 65, 66]. In this study, desirability was equivalent to 1 for tensile strengths of all the developed composites. Individual and overall desirability, as well as accruing tensile strengths of the developed fiber-reinforced PLA composites, are shown in Figs. 12b – 15b and 12c – 15c respectively. Moreover,

experiments were conducted to validate the optimal conditions that were determined by statistical modeling. As such, fiber-reinforced PLA composite samples were prepared according to the ramp suggestions in Figs. 12a–15a and the response (tensile strength) was obtained experimentally. The obtained results showed that the actual values of tensile strength were closely related with the predicted values showed in the tensile strength cubes (see Figs. 12c–15c). The percentage errors between the actual and predicted values were 1.12%, 1.87%, 1.39%, and 2.72% for PLA/clay composites loaded with NaOH-modified K85 rice husks, $\text{Mg}(\text{OH})_2$ -modified K85 rice husks, NaOH-modified K98 rice husks, and $\text{Mg}(\text{OH})_2$ -modified K98 rice husks respectively. This suggested that the models' adequacies were reasonable and hence validity was confirmed [35, 46, 63]. Additionally, the results obtained in each set of composites

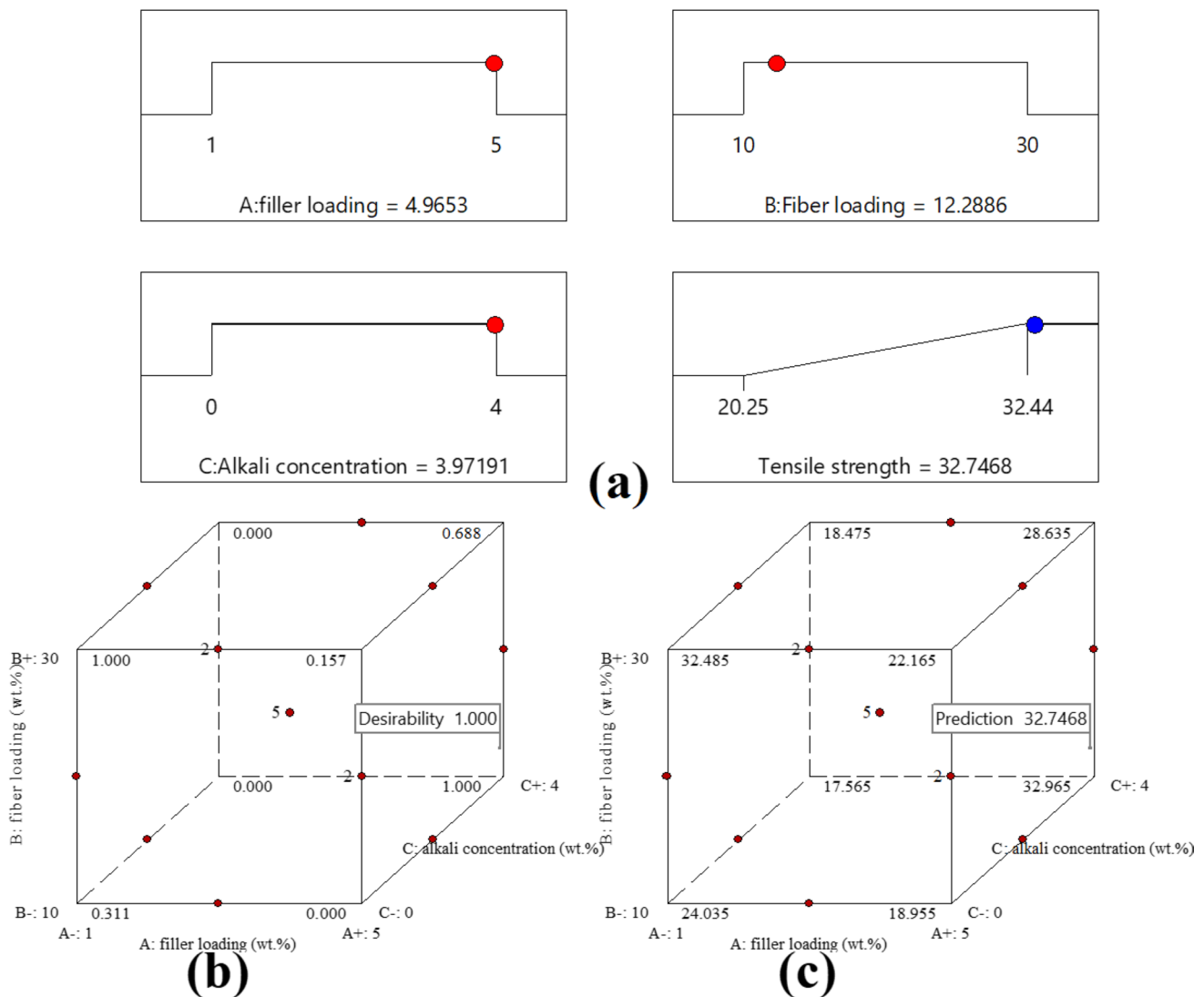


Fig. 15 Typical (a) ramp, (b) desirability cube, (c) tensile strength cube for optimization of filler loading, fiber loading, and alkali modification for PLA/clay/ $\text{Mg}(\text{OH})_2$ -modified K98 rice husks

are acceptable, indicating that a BBD is a very effective tool for optimizing individual factors in a new process.

4 Conclusions

This study optimized blending parameters of PLA/clay/rice husk composites through response surface methodology (RSM). The effect of clay filler loading, rice husk fiber loading, alkali concentration, rice husk variety, and alkali type on tensile strengths of the developed composites was evaluated using Box-Behnken design (BBD). Clay filler loading was found to exhibit the greatest influence on tensile strength of the developed PLA/clay/rice husk composites. The interaction effect was found to be more predominant than the linear and quadratic effects for tensile strength. The total percentage contributions (TPC) for interaction effects were 83.42%, 77.27%, 71.96%, and 81.94% for PLA/clay composites loaded with NaOH-modified K85 rice husks, Mg(OH)₂-modified K85 rice husks, NaOH-modified K98 rice husks, and Mg(OH)₂-modified K98 rice husks respectively. Meanwhile, quadratic effects between factors were least predominant at 2.19%, 6.11%, 6.03%, and 4.14% respectively. The results showed good agreement between tensile strength experimental and predicted values for R^2 , predicted R^2 , and adjusted R^2 . The predicted tensile strengths were 32.09 MPa, 33.69 MPa, 32.47 MPa, and 32.75 MPa for PLA/clay composites loaded with NaOH-modified K85 rice husks, Mg(OH)₂-modified K85 rice husks, NaOH-modified K98 rice husks, and Mg(OH)₂-modified K98 rice husks respectively, which were very close to the obtained experimental values of 31.73 MPa, 33.06 MPa, 32.02 MPa, and 31.86 MPa respectively. The software's reliability was therefore validated since the errors in tensile strengths between the actual and predicted optimized composites were relatively low. The present paper has shown that the BBD method is an economical way of gathering optimum values of tensile strength of PLA/clay/rice husk composites in the shortest period of time. This type of study is extremely promising because it is the first step to building a synergy between waste materials and their utilization in Uganda's automotive industry.

Acknowledgements Technical support from Yosevi Engineering Services Limited, www.yosevi.com, is gratefully acknowledged.

Author contribution Mr. Vianney Andrew Yiga—conceptualization, experimentation, data analysis, writing-original draft, technical editing. Dr. Michael Lubwama—conceptualization, experimentation, supervision, fund acquisition. Ms. Sinja Pagel—writing-original draft, technical editing, investigation. Dr. Peter Wilberforce Olupot—experimentation, technical editing, investigation. Dr. -Ing. Johannes Benz—conceptualization, technical editing. Prof. Christian Bonten—conceptualization, technical editing, supervision.

Funding This work was financially supported by the Volkswagen Foundation under grant no. 96655 entitled “Enhanced flame retardancy of bio-composite plastics developed with rice husks and clay fillers.”

Declarations

Conflict of interest The authors declare no competing interests.

Open Access This article is licensed under a Creative Commons Attribution 4.0 International License, which permits use, sharing, adaptation, distribution and reproduction in any medium or format, as long as you give appropriate credit to the original author(s) and the source, provide a link to the Creative Commons licence, and indicate if changes were made. The images or other third party material in this article are included in the article's Creative Commons licence, unless indicated otherwise in a credit line to the material. If material is not included in the article's Creative Commons licence and your intended use is not permitted by statutory regulation or exceeds the permitted use, you will need to obtain permission directly from the copyright holder. To view a copy of this licence, visit <http://creativecommons.org/licenses/by/4.0/>.

References

1. Nishata RRR, Sulong AB, Yuliana NY, Sahrim A (2017) Effect of surface modified rice husk (RH) on the flexural properties of recycled HDPE/RH composite. *Advances in Materials and Processing Technologies* 3(4):482–489. <https://doi.org/10.1080/2374068X.2017.1340420>
2. Chen S, Hori N, Kajiyama M, Takemura A (2020) Compatibilities and properties of poly lactide/poly (methyl acrylate) grafted chicken feather composite: effects of graft chain length. *J Appl Polym Sci* 137(34):48981. <https://doi.org/10.1002/app.48981>
3. Chen RS, Ahmad S (2017) Mechanical performance and flame retardancy of rice husk/organoclay-reinforced blend of recycled plastics. *Mater Chem Phys* 198:57–65. <https://doi.org/10.1016/j.matchemphys.2017.05.054>
4. Jain N, Verma A, Singh VK (2019) Dynamic mechanical analysis and creep-recovery behaviour of polyvinyl alcohol based cross-linked biocomposite reinforced with basalt fiber. *Materials Research Express* 6(10):105373. <https://doi.org/10.1088/2053-1591/ab4332>
5. Siakeng R, Jawaid M, Ariffin H, Sapuan SM (2019) Mechanical, dynamic, and thermomechanical properties of coir/pineapple leaf fiber reinforced polylactic acid hybrid biocomposites. *Polym Compos* 40(5):2000–2011. <https://doi.org/10.1002/pc.24978>
6. Verma A, Gaur A, Singh VK (2017) Mechanical properties and microstructure of starch and sisal fiber biocomposite modified with epoxy resin. *Materials Performance and Characterization* 6(1):500–520. <https://doi.org/10.1520/MPC20170069>
7. Yiga VA, Lubwama M, Pagel S, Benz J, Olupot PW, Bonten C (2021) Flame retardancy and thermal stability of agricultural residue fiber-reinforced polylactic acid: a Review. *Polym Compos* 42(1):15–44. <https://doi.org/10.1002/pc.25835>
8. Norhasnan NHA, Hassan MZ, Nor AFM, Zaki SA, Dolah R, Jamaludin KR, Aziz SAA (2021) Physicomechanical properties of rice husk/coco peat reinforced acrylonitrile butadiene styrene blend composites. *Polymers* 13(7):1171. <https://doi.org/10.3390/polym13071171>
9. Bariani, M., Boix, E., Cassella, F., & Cabrera, M. N. (2020). Furfural production from rice husks within a biorefinery

- framework Biomass Convers Biorefin 14 <https://doi.org/10.1007/s13399-020-00810-1>
10. Premalal HG, Ismail H, Baharin A (2002) Comparison of the mechanical properties of rice husk powder filled polypropylene composites with talc filled polypropylene composites. *Polym Testing* 21(7):833–839. [https://doi.org/10.1016/S0142-9418\(02\)00018-1](https://doi.org/10.1016/S0142-9418(02)00018-1)
 11. Menya E, Olupot PW, Storz H, Lubwama M, Kiros Y (2018) Characterization and alkaline pretreatment of rice husk varieties in Uganda for potential utilization as precursors in the production of activated carbon and other value-added products. *Waste Manage* 81:104–116. <https://doi.org/10.1016/j.wasman.2018.09.050>
 12. Yiga VA, Pagel S, Lubwama M, Epple S, Olupot PW, Bonten C (2020) Development of fiber-reinforced polypropylene with NaOH pretreated rice and coffee husks as fillers: mechanical and thermal properties. *J Thermoplast Compos Mater* 33(9):1269–291. <https://doi.org/10.1177/2F0892705718823255>
 13. Musinguzi TL, Yiga VA, Lubwama M (2019) Production of biocomposite polymers with rice and coffee husks as reinforcing fillers using a low-cost compression molding machine. *J Eng Agriculture Environment*. 5(1):61–72. <https://doi.org/10.37017/jae-vol5-no1.2019-5>
 14. Lubwama M, Yiga VA (2018) Characteristics of briquettes developed from rice and coffee husks for domestic cooking applications in Uganda. *Renewable Energy* 118:43–55. <https://doi.org/10.1016/j.renene.2017.11.003>
 15. Hamdan MM, Siregar JP, Rejab MRM, Bachtiar D, Jamiluddin J, Tezara C (2019) Effect of maleated anhydride on mechanical properties of rice husk filler reinforced PLA matrix polymer composite. *Int J Precis Eng Manufacturing-Green Technol* 6(1):113–124. <https://doi.org/10.1007/s40684-019-00017-4>
 16. Adeosun SO, Aworinde AK, Diwe IV, Olaleye SA (2016) Mechanical and microstructural characteristics of rice husk reinforced polylactide nano composite. *The West Indian J Eng* 39(1):63–71
 17. Pradeep, S. A., Iyer, R. K., Kazan, H., & Pilla, S. (2017). Automotive applications of plastics: past, present, and future. In *Applied Plastics Engineering Handbook* (651–673). William Andrew Publishing. <https://doi.org/10.1016/B978-0-323-39040-8.00031-6>
 18. Rwwiire S, Tomkova B, Militky J, Jabbar A, Kale BM (2015) Development of a biocomposite based on green epoxy polymer and natural cellulose fabric (bark cloth) for automotive instrument panel applications. *Compos B Eng* 81:149–157. <https://doi.org/10.1016/j.compositesb.2015.06.021>
 19. Kovacevic Z, Bischof S, Fan M (2015) The influence of Spartium junceum L. fibres modified with montmorillonite nanoclay on the thermal properties of PLA biocomposites. *Compos B Eng* 78:122–130. <https://doi.org/10.1016/j.compositesb.2015.02.034>
 20. Wang, H., Memon, H., Hassan, E. A., Elagib, T. H., Hassan, F. E. A., & Yu, M. (2019). Rheological and dynamic mechanical properties of abutilon natural straw and polylactic acid biocomposites. *Int J Polymer Sci* 2019 <https://doi.org/10.1155/2019/8732520>
 21. Yu T, Jiang N, Li Y (2014) Study on short ramie fiber/poly (lactic acid) composites compatibilized by maleic anhydride. *Compos A Appl Sci Manuf* 64:139–146. <https://doi.org/10.1016/j.compositesa.2014.05.008>
 22. Sajna VP, Mohanty S, Nayak SK (2014) Hybrid green nanocomposites of poly (lactic acid) reinforced with banana fibre and nanoclay. *J Reinf Plast Compos* 33(18):1717–1732. <https://doi.org/10.1177/2F0731684414542992>
 23. Mohammed L, Ansari MN, Pua G, Jawaid M, Islam MS (2015) A review on natural fiber reinforced polymer composite and its applications. *Int J Polymer Sci*. <https://doi.org/10.1155/2015/243947>
 24. Jandas PJ, Mohanty S, Nayak SK (2013) Surface treated banana fiber reinforced poly (lactic acid) nanocomposites for disposable applications. *J Clean Prod* 52:392–401. <https://doi.org/10.1016/j.jclepro.2013.03.033>
 25. Hassan, M. Z., Roslan, S. A., Sapuan, S. M., Rasid, Z. A., Mohd Nor, A. F., Md Daud, M. Y., ... & Mohamed Yusoff, M. Z. (2020). Mercerization optimization of bamboo (*bambusa vulgaris*) fiber-reinforced epoxy composite structures using a box–behnen design. *Polymers* 12 6 1367 <https://doi.org/10.3390/polym12061367>
 26. Hu G, Cai S, Zhou Y, Zhang N, Ren J (2018) Enhanced mechanical and thermal properties of poly (lactic acid)/bamboo fiber composites via surface modification. *J Reinf Plast Compos* 37(12):841–852. <https://doi.org/10.1177/2F0731684418765085>
 27. Ramesh, P., Prasad, B. D., & Narayana, K. L. (2019). Effect of MMT Clay on mechanical, thermal and barrier properties of treated aloevera fiber/PLA-hybrid biocomposites. *SILICON* 1–10 <https://doi.org/10.1007/s12633-019-00275-6>
 28. Eng, C. C., Ibrahim, N. A., Zainuddin, N., Ariffin, H., Yunus, W. M., Wan, Z., & Then, Y. Y. (2014). Enhancement of mechanical and dynamic mechanical properties of hydrophilic nanoclay reinforced polylactic acid/polycaprolactone/oil palm mesocarp fiber hybrid composites. *Int J Polymer Sci* 2014 <https://doi.org/10.1155/2014/715801>
 29. Kumar R, Yakabu MK, Anandjiwala RD (2010) Effect of montmorillonite clay on flax fabric reinforced poly lactic acid composites with amphiphilic additives. *Compos A Appl Sci Manuf* 41(11):1620–1627. <https://doi.org/10.1016/j.compositesa.2010.07.012>
 30. Tharazi, I., Sulong, A. B., Muhamad, N., Haron, C. H. C., Tholibon, D., Ismail, N. F., ... & Razak, Z. (2017). Optimization of hot press parameters on tensile strength for unidirectional long kenaf fiber reinforced polylactic-acid composite. *Procedia Engineering* 184 478 485 <https://doi.org/10.1016/j.proeng.2017.04.150>
 31. Menya E, Olupot PW, Storz H, Lubwama M, Kiros Y, John MJ (2020) Optimization of pyrolysis conditions for char production from rice husks and its characterization as a precursor for production of activated carbon. *Biomass Convers Biorefin* 10(1):57–72. <https://doi.org/10.1007/s13399-019-00399-0>
 32. Biswas S, Bal M, Behera SK, Sen TK, Meikap BC (2019) Process optimization study of Zn²⁺ adsorption on biochar-alginate composite adsorbent by response surface methodology (RSM). *Water* 11(2):325. <https://doi.org/10.3390/w11020325>
 33. Saba N, Allothman OY, Almutairi Z, Jawaaid M (2019) Magnesium hydroxide reinforced kenaf fibers/epoxy hybrid composites: mechanical and thermomechanical properties. *Constr Build Mater* 201:138–148. <https://doi.org/10.1016/j.conbuildmat.2018.12.182>
 34. Yiga VA, Lubwama M, Olupot PW (2021) Effect of alkaline surface modification and carbonization on biochemical properties of rice and coffee husks for use in briquettes and fiber-reinforced plastics. *J Nat Fibers* 18(4):620–629. <https://doi.org/10.1080/15440478.2019.1642824>
 35. Hassan MZ, Sapuan SM, Roslan SA, Sarip S (2019) Optimization of tensile behavior of banana pseudo-stem (*Musa acuminata*) fiber reinforced epoxy composites using response surface methodology. *J Market Res* 8(4):3517–3528. <https://doi.org/10.1016/j.jmrt.2019.06.026>
 36. Chaker H, Ameur N, Saidi-Bendahou K, Djennas M, Fourmentin S (2021) Modeling and Box-Behnken design optimization of photocatalytic parameters for efficient removal of dye by lanthanum-doped mesoporous TiO₂. *J Environ Chem Eng* 9(1):104584. <https://doi.org/10.1016/j.jece.2020.104584>
 37. Phua YJ, Pegoretti A, Mohd Ishak ZA (2018) Experimental analysis and theoretical modeling of the mechanical behavior of starch-grafted-polypropylene/kenaf fibers composites. *Polym Compos* 39(9):3289–3299. <https://doi.org/10.1002/pc.24344>
 38. Chaker H, Attar AE, Djennas M, Fourmentin S (2021) A statistical modeling-optimization approach for efficiency photocatalytic degradation of

- textile azo dye using cerium-doped mesoporous ZnO: a central composite design in response surface methodology. *Chem Eng Res Des* 171:198–212. <https://doi.org/10.1016/j.cherd.2021.05.008>
39. Montgomery, D. C. (2017). *Design and analysis of experiments*. John Wiley & sons.
 40. Haji A (2017) Improved natural dyeing of cotton by plasma treatment and chitosan coating; optimization by response surface methodology. *Cellul Chem Technol* 51(9–10):975–982
 41. Chaker H, Ferouani G, Chikhi I, Djennas M, Fourmentin S (2021) A novel statistical approach for the synthesis of Chalcones via Claisen-Schmidt condensation catalyzed by Pd nanoparticles modified mesoporous TiO₂ as an efficient heterogeneous catalyst. *Colloids Interface Sci Commun* 43:100461. <https://doi.org/10.1016/j.colcom.2021.100461>
 42. Lubwama, M., Yiga, V. A., & Lubwama, H. N. (2020). Effects and interactions of the agricultural waste residues and binder type on physical properties and calorific values of carbonized briquettes. *Biomass Convers Biorefin* 1–21. <https://doi.org/10.1007/s13399-020-01001-8>
 43. Yaghoobi H, Fereidoon A (2018) Modeling and optimization of tensile strength and modulus of polypropylene/kenaf fiber biocomposites using Box-Behnken response surface method. *Polym Compos* 39:E463–E479. <https://doi.org/10.1002/pc.24596>
 44. Shokrollahi M, Rezakazemi M, Younas M (2020) Producing water from saline streams using membrane distillation: modeling and optimization using CFD and design expert. *Int J Energy Res* 44(11):8841–8853. <https://doi.org/10.1002/er.5578>
 45. Chen C, Shao Y, Tao Y, Wen H (2015) Optimization of dynamic microwave-assisted extraction of *Armillaria polysaccharides* using RSM, and their biological activity. *LWT-Food Science and Technology* 64(2):1263–1269. <https://doi.org/10.1016/j.lwt.2015.07.009>
 46. Nor, A. F. M., Hassan, M. Z., Rasid, Z. A., Sarip, S., & Daud, M. Y. M. (2021). Optimization on tensile properties of kenaf/multi-walled CNT hybrid composites with Box-Behnken design. *Appl Compos Mater* 1–26. <https://doi.org/10.1007/s10443-021-09879-x>
 47. Pavani S, Rao YM, Kumar YS (2016) Use of Box-Behnken experimental design for optimization of process variables in iontophoretic delivery of repaglinide. *J Young Pharm* 8(4):350. <https://doi.org/10.5530/jyp.2016.4.10>
 48. Stamenković OS, Kostić MD, Radosavljević DB, Veljković VB (2018) Comparison of box-behnken, face central composite and full factorial designs in optimization of hempseed oil extraction by n-hexane: a case study. *Periodica Polytech, Chem Eng* 62(3):359–367. <https://doi.org/10.3311/PPch.11448>
 49. Omulo G, Banadda N, Kabenge I, Seay J (2019) Optimizing slow pyrolysis of banana peels wastes using response surface methodology. *Environmental Engineering Research* 24(2):354–361. <https://doi.org/10.4491/eer.2018.269>
 50. Chowdhury ZZ, Yehye WA, Julkapli NM, Al Saadi MAH, Atieh MA (2016) Application of graphitic bio-carbon using two-level factorial design for microwave-assisted carbonization. *BioResources* 11(2):3637–3659
 51. Awolusi TF, Oke OL, Akinkulore OO, Sojobi AO (2019) Application of response surface methodology: predicting and optimizing the properties of concrete containing steel fibre extracted from waste tires with limestone powder as filler. *Case studies in Construction materials* 10:e00212. <https://doi.org/10.1016/j.cscm.2018.e00212>
 52. Tawakkal IS, Cran MJ, Bigger SW (2014) Effect of kenaf fibre loading and thymol concentration on the mechanical and thermal properties of PLA/kenaf/thymol composites. *Ind Crops Prod* 61:74–83. <https://doi.org/10.1016/j.indcrop.2014.06.032>
 53. King FL, Kumar AJ, A., & Vijayaraghavan, S. (2019) Mechanical characterization of polylactic acid reinforced bagasse/basalt hybrid fiber composites. *J Compos Mater* 53(1):33–43. <https://doi.org/10.1177/0021998318780208>
 54. Ibrahim NA, Yunus WMZW, Othman M, Abdan K, Hadithon KA (2010) Poly (lactic acid)(PLA)-reinforced kenaf bast fiber composites: the effect of triacetin. *J Reinf Plast Compos* 29(7):1099–1111. <https://doi.org/10.1177/2F0731684409344651>
 55. Ng, Y. R., Shahid, S. N. A. M., & Nordin, N. I. A. A. (2018, June). The effect of alkali treatment on tensile properties of coir/polypropylene biocomposite. In *IOP Conference Series: Materials Science and Engineering* (Vol. 368, No. 1, p. 012048). IOP Publishing. <https://doi.org/10.1088/1757-899X/368/1/012048>
 56. Ramesh P, Prasad BD, Narayana KL (2020) Effect of fiber hybridization and montmorillonite clay on properties of treated kenaf/aloë vera fiber reinforced PLA hybrid nanobiocomposite. *Cellulose* 27:6977–6993. <https://doi.org/10.1007/s10570-020-03268-6>
 57. Fan Q, Han G, Cheng W, Tian H, Wang D, Xuan L (2018) Effect of intercalation structure of organo-modified montmorillonite/poly(lactic acid) on wheat straw fiber/poly(lactic acid) composites. *Polymers* 10(8):896. <https://doi.org/10.3390/polym10080896>
 58. Ramesh, P., Prasad, B. D., & Narayana, K. L. (2019, January). Morphological and mechanical properties of treated kenaf fiber/MMT clay reinforced PLA hybrid biocomposites. In *AIP Conference Proceedings* (Vol. 2057, No. 1, p. 020035). AIP Publishing LLC. <https://doi.org/10.1063/1.5085606>
 59. Ouajai, S., & Phongtamrug, S. (2020). Morphological, thermal and mechanical properties of poly (lactic acid)/cellulose/nano-clay composite. In *Key Engineering Materials* (Vol. 856, pp. 331–338). Trans Tech Publications Ltd. <https://doi.org/10.4028/www.scientific.net/KEM.856.331>
 60. Zhang, K., Lin, J., Hao, C., Hong, G., Chen, Z., Chen, Z., ... & Song, W. (2019). Effect of nano-hydroxyapatite modification of bamboo fiber on the properties of bamboo fiber/poly(lactic acid) composites. *BioResources*, 14(1), 1694–1707. <https://doi.org/10.15376/biores.14.1.1694-1707>
 61. Usman A, Sutanto MH, Napiah M, Zoorob SE, Abdulrahman S, Saeed SM (2021) Irradiated polyethylene terephthalate fiber and binder contents optimization for fiber-reinforced asphalt mix using response surface methodology. *Ain Shams Engineering Journal* 12(1):271–282. <https://doi.org/10.1016/j.asej.2020.06.011>
 62. Nurkhoeriyati T, Kulig B, Sturm B, Hensel O (2021) The effect of pre-drying treatment and drying conditions on quality and energy consumption of hot air-dried celeriac slices: optimisation. *Foods* 10(8):1758. <https://doi.org/10.3390/foods10081758>
 63. Siddique, S. H., Faisal, S., Ali, M., & Gong, R. H. (2020). Optimization of process variables for tensile properties of bagasse fiber-reinforced composites using response surface methodology. *Polym Polym Compos*, 0967391120968432. <https://doi.org/10.1177/2F0967391120968432>
 64. Aldahdooh MAA, Bunnori NM, Johari MM (2013) Evaluation of ultra-high-performance-fiber reinforced concrete binder content using the response surface method. *Mater Des* 1980–2015(52):957–965. <https://doi.org/10.1016/j.matdes.2013.06.034>
 65. de Araújo Morandim-Giannetti A, Pasquoto CG, Sombra TM, Bonse BC, Bettini SHP (2018) Polypropylene/chemically treated coir composites: optimizing coir delignification conditions using central composite design. *Cellulose* 25(2):1159–1170. <https://doi.org/10.1007/s10570-017-1617-y>
 66. Chamoli S (2015) ANN and RSM approach for modeling and optimization of designing parameters for a V down perforated baffle roughened rectangular channel. *Alex Eng J* 54(3):429–446. <https://doi.org/10.1016/j.aej.2015.03.018>